NASA TECHNICAL MEMORANDUM

NASA TM X-2987

NASA TM X-2987

EFFLUENT SAMPLING OF SCOUT "D" AND DELTA LAUNCH VEHICLE EXHAUSTS

by William C. Hulten, Richard W. Storey, Gerald L. Gregory, David C. Woods, and Franklin S. Harris, Jr.

Langley Research Center
Hampton, Va. 23665

NATIONAL AERONAUTICS AND SPACE ADMINISTRATION • WASHINGTON, D. C. • JULY 1974

1. Report No.	2. Government Accession No.	3. Recipient's Catalog No.
NASA TM X-2987		

4. Title and Subtitle	5. Report Date
EFFLUENT SAMPLING OF SCOUT "D" AND DELTA LAUNCH VEHICLE EXHAUSTS	July 1974
	6. Performing Organization Code

7. Author(s)	8. Performing Organization Report No.
William C. Hulten, Richard W. Storey, Gerald L. Gregory, David C. Woods, and Franklin S. Harris, Jr.	L-9360
	10. Work Unit No.
9. Performing Organization Name and Address	909-72-47-01
NASA Langley Research Center Hampton, Va. 23665	11. Contract or Grant No.
	13. Type of Report and Period Covered
12. Sponsoring Agency Name and Address	Technical Memorandum
National Aeronautics and Space Administration Washington, D.C. 20546	14. Sponsoring Agency Code

15. Supplementary Notes

William C. Hulten, deceased.

Franklin S. Harris, Jr., is a research professor in the Department of Physics, Geophysical Sciences, and Oceanography at Old Dominion University, Norfolk, Virginia.

16. Abstract

Characterization of engine-exhaust effluents (hydrogen chloride, aluminum oxide, carbon dioxide, and carbon monoxide) has been attempted by conducting field experiments monitoring the exhaust cloud from a Scout-Algol III vehicle launch and a Delta-Thor vehicle launch. The exhaust cloud particulate size number distribution (total number of particles as a function of particle diameter), mass loading, morphology, and elemental composition have been determined within limitations. The gaseous species in the exhaust cloud have been identified. In addition to the ground-based measurements, instrumented aircraft flights through the low-altitude, stabilized-exhaust cloud provided measurements which identified CO and HCl gases and Al_2O_3 particles. Measurements of the initial exhaust cloud during formation and downwind at several distances have established sampling techniques which will be used for experimental verification of model predictions of effluent dispersion and fallout from exhaust clouds.

17. Key Words (Suggested by Author(s))	18. Distribution Statement
Effluent sampling Vehicle exhaust Particle sampling Gaseous measurements	Unclassified – Unlimited STAR Category 31

19. Security Classif. (of this report)	20. Security Classif. (of this page)	21. No. of Pages	22. Price*
Unclassified	Unclassified	69	$3.75

*For sale by the National Technical Information Service, Springfield, Virginia 22151

EFFLUENT SAMPLING OF SCOUT "D" AND DELTA LAUNCH VEHICLE EXHAUSTS

By William C. Hulten,* Richard W. Storey, Gerald L. Gregory,
David C. Woods, and Franklin S. Harris, Jr.**
Langley Research Center

SUMMARY

Characterization of engine-exhaust effluents (hydrogen chloride, aluminum oxide, carbon dioxide, and carbon monoxide) has been attempted by conducting field experiments monitoring the exhaust cloud from a Scout-Algol III vehicle launch and a Delta-Thor vehicle launch. The exhaust cloud particulate size number distribution (total number of particles as a function of particle diameter), mass loading, morphology, and elemental composition have been determined within limitations. The gaseous species in the exhaust cloud have been identified. In addition to the ground-based measurements, instrumented aircraft flights through the low-altitude, stabilized-exhaust cloud provided measurements which identified CO and HCl gases and Al_2O_3 particles. Measurements of the initial exhaust cloud during formation and downwind at several distances have established sampling techniques which will be used for experimental verification of model predictions of effluent dispersion and fallout from exhaust clouds.

INTRODUCTION

The use of rockets in future NASA launch operations requires a study of the possible climatic impact of the exhausts. Such a study will include measuring the rocket effluents – both particulate and gaseous – from solid rocket engine exhausts. This report describes the sampling techniques and the instrumentation used for making such measurements from two rocket launches. These measurements were not intended to be comprehensive but only to serve as a feasibility study to establish techniques and procedures for follow-on experiments. The techniques used in these measurements were restricted to in-house availability of instruments at the time.

A discussion of particle measuring systems is presented in appendix A. Gaseous measuring systems are discussed in appendix B and particulate elemental analysis techniques are presented in appendix C.

---

*William C. Hulten, deceased.

**Franklin S. Harris, Jr., is a research professor in the Department of Physics, Geophysical Sciences, and Oceanography at Old Dominion University, Norfolk, Virginia.

EXPERIMENTAL PROCEDURE

It has been established (ref. 1) that low-altitude clouds of motor exhaust and entrained gases are formed during the launch of the Scout vehicle. These clouds rise and stabilize at an altitude of approximately 400 meters depending upon meteorological conditions. For a cloud stabilization altitude of 400 meters, the ground cloud contains the exhaust effluents produced during the first 8 seconds of motor ignition. The exhaust products at the exit of the Scout first-stage motor which were investigated are as follows (the measurements were made in the stabilized ground cloud):

Products	Percent by weight
Al_2O_3	32.1
CO	27.4
HCl	20.6
CO_2	21.1

The Delta launch vehicle studied consisted of a liquid-fuel engine and six solid-fuel strap-on engines. The fuel composition of the Delta first stage is given in percent by weight (from ref. 2).

Composition	Percent by weight
CO (liquid-fuel engine)	47.30
CO (solid-fuel engine)	22.26
HCl	20.83
Al_2O_3	37.77

The measurement systems used for the gaseous and the particulate products in the engine exhausts are described.

Particulate Measuring System

The high volume, Andersen, Lundgren, and membrane filter particulate impaction systems were used for the time-integrated filter sampling. The real-time sampling utilized the Royco and Climet light-scattering photometers and the mass monitor. Samples collected by the mass monitor and the filters could be analyzed later for elemental composition by using techniques described in appendix C. The instruments were operated before, during, and after the launch to differentiate between atmospheric background and launch effluents. A brief description of each type of instrument used for particulate sampling is included in appendix A.

Gaseous Measurement System

The gaseous measurement system included evacuated gas grab samplers for CO and CO_2.

Microcoulometers, M-S-A portable Billion-Aire analyzers, and distilled water bubblers were used for HCl detection (Delta launch only). In addition, pH paper was used at each of the sites for qualitative indication of HCl. The aircraft instrumentation consisted of pH paper, a mass spectrometer, grab samplers (Scout launch only), and an infrared CO detector (Delta launch only). Additional discussion of the gaseous measurement system is given in appendix B.

EXPERIMENTAL RESULTS

Preliminary measurements were made of the exhaust effluents from the Scout D vehicle during the launch of the Meteoroid Technology Satellite and the Delta vehicle during the launch of the Telsat-A satellite. The Scout vehicle was launched from Wallops Island, Virginia, at 11:10 a.m. e.d.t., August 13, 1972. The Delta vehicle was launched from Kennedy Space Center (KSC) at 8:14 p.m. e.s.t., November 9, 1972.

Selection of Monitoring Sites for the Scout Launch

For the Scout launch, ground-level monitoring site locations were selected 2 months prior to launch, based on the most probable wind direction at launch time. Prevailing wind direction data for the area and minimal photographic coverage of prior launches were used in site selection. Additional sites were selected to cover other wind directions. Ground sites were located primarily to obtain effluent measurements during cloud formation. Aircraft effluent measurements were directed at effluent dispersion and diffusion in the cloud. The Scout particulate monitoring instrumentation sites are shown in figures 1 and 2 and in table I. The gaseous monitoring sites are shown in figure 3.

Scout Particulate Size Distribution Results

The Royco light-scattering photometer located at sampling site 1 (fig. 1) provided the only real-time particle-size distribution data during launch as shown in figure 4. The time shown for each curve is the start of a particle sampling collection interval of 1 minute. The solid curve at time 11:07:54 is representative of prelaunch background conditions where no appreciable change in the natural background data was noted for several hours before the launch. The size distribution curve for the time 11:10:32 shows a sudden radical change at 32 seconds after the launch. The curves for times up to 9 minutes after launch show successive decreases toward the return to natural atmospheric background.

Because of the large number of particles produced in the atmosphere during the launch, the Royco instrument was providing a distorted size distribution brought on by

coincidence problems due to the presence of more than one particle in the counting volume at the same time. This condition would result in too low values for the number of small particles. The dip in the curve for time 11:10:32 around 1.3 μm indicates this coincidence condition and that many of the smaller particles were coincident with larger particles and hence not individually counted. The horizontal part of the same curve does not show definite indications of convergence or dropping off; therefore, there must have been large particles above 6 μm diameter which were not measured because of the instrumentation upper-sizing limitations of 6 μm. Without a coincidence correction, one may conclude an average of three orders of magnitude increase in the number of particles 3 to 6 μm in diameter resulting from the launch. Another way of presenting these distribution data is shown in figure 5. The number of particles were converted to mass by assuming a density of 2.3 g/cm^3 (for Al_2O_3), multiplying by the mean volume of each particle in a size interval, and the number of particles in that size. The sizes were then grouped together as shown on the plot. As one would expect, the mass loading followed the particle size distribution pattern of an apparent drop in material in the smaller size ranges and large increases due to the larger particles.

Time-integrated sampling at each of two sites 7 and 8 with the Andersen aerodynamic sizing section on the high-volume sampler provided the data plotted in figure 6. This is a log probability plot with the cumulative percentage of mass less than indicated size plotted against the mean aerodynamic size for each stage of the sampling section. If the distribution is log-normal, it would be a straight line. This seems to be the case within the limitations of the small differences in mass obtained in weighing of the filters. The data agree with Royco measurements which show that the effluents from the rocket produced relatively more large particles in the atmosphere. The difference between the two launch curves may be explained by their difference in distance from the rocket. Site 8 was farther away and did not have the same exposure to the ground cloud as site 7. The Titan curve is based on samples collected from an aircraft during static test firings of the Titan rocket. Particles smaller than 3 μm were not counted. A direct data comparison is not expected because of the different rockets and sample collection methods and conditions; however, the same trends in the data are significant.

The Andersen eight-stage impactor which collects particles according to their aerodynamic dimensions was used at several monitoring sites. Only stages 3 and 4 were equipped with glass plates to provide some preliminary particle counting information; on other stages, suitable substrates were used for elemental analysis. (To obtain a complete size distribution from the Andersen impactor, the particles must be counted in all stages, not just the total particles in each stage, but the actual distribution in each stage.) Figure 7 shows the distribution during launch at site 3 for the particles collected by the Andersen third stage. The actual particles collected in a given stage include a considerable number larger and smaller than the nominal range for the stage (3.3 to 4.7 μm for

50-percent cut points). Figure 7 presents the number of particles counted per class interval of equal linear diameter widths because the actual counting was carried out in linear rather than logarithmic increments. A log-normal plot would remove the asymmetry and for the whole size range a dN/d log D variation with log D often gives the best representation.

Particles collected by the Andersen sampler at the downwind site 3, along the exhaust cloud path were compared with the prelaunch and postlaunch natural atmospheric background particulates. The mean particle diameter collected at site 3 on the Andersen sampler stage 3 was 3.85 μm ± 1.88 μm; by comparison, the background mean diameter was 4.25 μm ± 2.72 μm. The smaller standard deviation during launch implies less scatter in the particles' sizing and suggests more uniformly shaped particles from the launch than the prelaunch and postlaunch background produced. This result has been further supported by analysis of the particles by use of the scanning electron microscope (SEM) which shows that the particles collected during the launch are spheres consisting predominantly of aluminum. Figure 8 shows the homogeneity of the particles collected on stage 3 at site 1 during the launch. The total collection time was 8 minutes. The photograph is by reflected bright field illumination with ×1600 magnification. As with this stage, it was not possible to count the particles collected on stages at all sites during the launch because they were too numerous and too close together to count. By comparison, figure 9 shows the postlaunch background particles; the total collection time was 5 hours. The photograph is by reflected bright field illumination with ×1600 magnification. The morphology of the particles between the two photographs is obviously different.

The Climet light-scattering photometer located at site 10 malfunctioned during the launch and only provided prelaunch and postlaunch background data.

Scout Particulate Mass Loading Results

The particulate mass loadings as determined by material collected on low-volume membrane filters and high-volume filters during and immediately following the launch are shown in figure 10. The center of the polar plot represents the Scout launch point. The ground wind was blowing from 175° at 9 knots. The upper winds which controlled the movement of the ground cloud were from 225°. The dark dots on the plot represent the site locations and the number beside each dot is the mass loading in $\mu g/m^3$. An elemental analysis of the collected material from a few select sites for aluminum was carried out and the amount is shown in parentheses. A background of 30 $\mu g/m^3$ was the average mass loading over 12-hour periods for the 3 days prior to launch and 1 day after launch. Mass loadings at four sites (location shown in fig. 10) during and immediately following launch collected on the membrane filters were as follows:

Site	Mass loading, $\mu g/m^3$	Time elapsed before switching off the instrument, min
1	12 300	8
10	477	17
11	160	40
12	148	50

The total collection time depended on when personnel could get to the site after the launch to turn off the instruments and is not associated with end of the cloud passage. The collection time included the launch effect but the mass loading represents an average over a longer period of time, and hence is not the maximum value. Because of the relatively short collection times, minutes during the launch as compared with hours for background data, a background correction for the launch data would be insignificant.

According to the ground cloud growth and direction of movement (45° at 400 meters altitude), the mass loadings at sites 7 and 1 should have resulted from direct sampling of the cloud. The data from sites 3, 11, and 12 should have included fallout from passage of the cloud.

The high-volume filter data taken before, during, and after the launch is shown in table II. The mass-loading values in the table are averaged over some minutes collection time during launch, but for prelaunch and postlaunch there were collection times of many hours. The arrows in the table indicate that for these values the collection period included parts of 2 days. The background measurements were not carried out under the same controlled conditions as during the launch when all activities in the area, which could have influenced the background data and not the launch data, were shut down. Thus, there was a difference in background from day to day.

Scout Particulate Analysis

The techniques for determining the elemental constituents of the collected samples are described in appendix C. Ten filter pads from Andersen samplers were examined by neutron activation analysis. The results of the analysis are presented in table III which lists the weight of each element found on the filter pads relative to a clean filter. The filters are identified by numbers preceded by the letter F and collection sites are given above these numbers. Filter F62 contained prelaunch material indicating background. Materials on filters F114 and F156 were collected postlaunch. All the other samples in the table were collected during launch. There was a significant amount of aluminum collected on F48 at site 1 relatively close to the launch site.

A scanning electron microscope (SEM) analysis of the Andersen filter pads from site 1 and aboard the aircraft during the launch showed the presence of aluminum particles. Figure 11 is an SEM photograph (×10 450 magnification) of the aluminum particles. The SEM spectra of these particles are shown in figure 12. The elemental constituents are determined from the position of the peaks. The high peak is due to aluminum and the two small peaks are due to the composition of the filter pads (as illustrated in fig. 12, a SEM analysis of an unused filter pad).

Figure 13 is an SEM photograph of particles collected at site 1 during launch. The spectra from these particles were observed to be the same, primarily aluminum. Figure 14 is a photograph emphasizing how some of the aluminum particles agglomerate. This collection was made on filter pad no. 48 which was also analyzed by using the neutron activation technique. Both methods gave the same results for this sample, which is a high percentage of aluminum.

Figure 15 shows a collection of material from the natural atmosphere made before launch. The SEM analysis indicated a trace of sodium, some aluminum, and a higher percentage of silicon. A postlaunch collection is shown in figure 16. Here again the SEM analysis shows some aluminum but a higher percentage of silicon. The amount of aluminum collected during launch was much greater than the amount collected prelaunch and postlaunch; also, the particles during launch were predominantly spheres.

Figure 17 shows an SEM picture of an unused filter pad. The two peaks are due to the elemental composition of the filter. The two peaks, phosphorous and chlorine, appear on all the scans where this type of filter was used.

Scout Gaseous Results

Postlaunch laboratory investigations of the validity of gas grab samples for detection of CO and CO_2 in the presence of HCl, Al_2O_3, and H_2O have shown this technique not to be valid for CO_2 detection. These studies have shown that CO_2 concentrations in the presence of HCl, Al_2O_3, and H_2O vary considerably with storage time and this variance is a function of many, yet to be defined, parameters. Thus, CO_2 measurements taken during the launch are not valid. However, the laboratory study did show that the gas grab sample technique is valid for CO detection. The limit of detection for CO was found to be 0.1 ppm with an accuracy about 10 percent of the indicated value. Storage times up to 1 week were investigated. The results for CO from the Scout launch are shown in table IV. The dashes in the table indicate that samples were not taken at that location at that time. Although the data in table IV do not present a complete picture of the exhaust cloud dynamics, it is important to note the following:

(1) At T + 5 seconds, all sites (except site 7) regardless of direction from the pad show an increase in CO concentration. This increase is most likely the result of the blast

effect from the launch, and thus is not wind dependent. The low concentrations could be the result of sample dilution if, for example, the launch effluent arrived at the sites toward the end of the sampling period. These samples were obtained over the time from T + 5 seconds to T + 7 seconds or T + 8 seconds.

(2) Site 7, 23 meters from the launch point, showed no increase in CO concentration from T + 0 seconds to T + 10 seconds. Instrumentation at site 7 was located on top of a one story building, and it is speculated that the building deflected the initial overpressure and prevented the collection of gaseous samples. That is, exhaust cloud pressures at the bottom of the wall vertically accelerated the effluents up the side of the building and over the instruments. This effect would be most pronounced for the gaseous species, thus, obtaining particulate samples at site 7 over significantly longer sampling periods is not inconsistent.

(3) The buildup of CO concentration at site 8 from T + 5 seconds to T + 60 seconds indicates the exhaust cloud is moving in that direction. In fact the 10.5 ppm CO indication at site 1 at T + 60 seconds as compared with the 14.8 ppm at site 8 would suggest that the cloud path (center line) is to the west of site 1. This general direction is further supported by the low CO concentrations at site 3 at T + 15 seconds and T + 30 seconds. It is also noted that the particulate data of figure 10 suggested a cloud movement in the direction of sites 1 and 8.

Figure 18 shows the results obtained from the pH sensitive papers. As shown in the figure and as explained in appendix B, the pH papers were grouped according to their color change: pH = 1, pH = 3, and "acid indication." As discussed in appendix B, those papers classed as "acid indication" are believed to be of questionable validity and will not be used to draw conclusions on HCl behavior. However, they are shown in figure 18 for reader interest and also serve to indicate the areas that were instrumented with pH papers. All pH paper sites except as indicated by the "line of no pH change" (fig. 18) showed some indication of acid being present. All pH papers were retrieved and individually sealed in plastic bags by T + 2 hours. As shown in the figure, the lower pH values (high acidity) were observed in the immediate vicinity of the launcher. The pH values of 3 were observed at farther distances from the launch pad. The important consideration is that pH values attributable to the launch were observed 300 to 400 meters from the launch vehicle, which is well beyond the initial ground effects from the rising vehicle.

Because of the limitations of the instrumentation, no data were obtained from the airborne sampling for gaseous species. Visible cloud penetrations by the aircraft were made, but the small size of the Scout cloud, the short duration of the cloud, and instrument response negated any meaningful results.

Selection of Monitoring Sites for the Delta Launch

For the Delta launch, the monitoring instrumentation and ground site locations were intended to concentrate on the measurement of effluent dispersion and fallout of the exhaust cloud after reaching stabilization altitude downwind of the launch point. The downwind site locations were chosen at T - 10 hours based on Marshall Space Flight Center cloud dispersion and meteorological predictions. Some 20 sites were available for selection ranging in all directions from the launch pad and at distances from about 0.5 to 5 km from the launch pad. Of these 20 sites, six were selected for instrumentation at T - 10 hours. These sites are shown in figure 19. One additional site (not shown in the figure) at 70° and 100 meters from the vehicle was instrumented. Table V shows the T - 10 hour predictions used in selecting the sites shown in figure 19. The wind direction was predicted to be from 035° (cloud heading, 215°) and this wind vector is shown in figure 19. At T - 3 hours, another prediction was supplied and is shown in table VI. The T - 3 hours prediction data were used to update the sampling procedures for the ground measurements and to finalize the airborne sampling plan. The airborne measurements were directed at obtaining effluent measurement in the stabilized ground cloud. As shown by comparison of table V and tables VI and VII, and T - 3 hours prediction indicated the same cloud heading, but showed a decrease in both the cloud ground speed and the concentrations of effluent reaching the ground. From the T - 3 hours prediction, new cloud arrival and passage times were calculated and furnished to personnel at sites R, S, and 1808. Site MAML was unmanned and no form of communication existed at sites O and Q.

Delta Particulate Measurement Results

Figure 20 shows the mass monitor results from site S, 3.18 km from the launch point in a downwind direction of 209°. The time change of the mass loading ($\mu g/m^3$) indicates the cloud arrival at site S approximately T + 14 minutes from launch as indicated by a greater than factor 3 increase in mass. The model predicted the cloud would arrive 3 km downwind on the 209° path at T + 13 minutes after launch. The natural atmospheric background before launch was in the range of 20 to 60 $\mu g/m^3$. Elemental analysis of the particles collected on the mass monitor crystal showed significant amounts of aluminum and is discussed later in this report.

Figure 21 shows the Climet light-scattering photometer measurements before, during, and after launch plotted in terms of mass loading in each of five channels where each channel represents a specific particle size range. The right-hand side of the curves were plotted in more detail for the times during and after which the cloud, moving with a predicted path direction of 215°, was expected to be over site R, 2.76 km at 225°. Since no significant change in the data occurred, it was concluded that the cloud did not pass over site R.

Figure 22 shows the Royco light-scattering photometer measurements conducted at site 1808, 5.25 km from the launch point at 217°. The 100 channels of data are grouped into four major particle size ranges and the mass loading calculated and plotted as a function of time. The arrival of the cloud at site 1808 approximately 23 minutes after launch is clearly evident by the change in particles which, it is to be noted, at this site was much more marked in the smaller sizes. Measurements were made for an hour after launch, although by that time the air at the site as seen from the plots had not yet returned to normal prelaunch background. Prelaunch model prediction data indicated that the cloud would be 5 km downwind on the 215° course at T + 23 minutes. Figure 23 shows the mass loading data from the Royco as a function of time as determined by the total number of particles measured in the size range of the instrument (0.6 to 6 μm).

Delta Particulate Size Distribution Results

The Royco data from site 1808 has been plotted in figure 24 in size number distributions as a function of time from launch. The 100 channels are grouped into four major size ranges. The cloud arrival is evident by the big increase in the number of particles at T + 23 minutes. The particle increase is more predominant in the smaller sizes.

Delta Particulate Analysis

The techniques for determining the elemental constituents of the collected samples are described in appendix C. The crystal from the mass monitor was examined with the scanning electron microscope (SEM). A group of photographs showing the particles analyzed with the SEM are shown in figures 25(a) and 25(b). The upper photograph in figure 25(a) shows a group of particles collected on the mass monitor located at site S, with magnification ×200. The three particles circled were selected for elemental analysis. Particle 1 is irregular in shape, 2 is spherical, and 3 has a cubical shape. The bottom photograph of figure 25(a) is a ×2000 magnification of particle 1. Since this particle was irregular in shape, scans were made at two separate locations on the particle (1-1 and 1-2). At 1-2 there appears to be a small particle which adhered to the large particle. The results of the analysis, as shown in table VIII, indicate that the elemental composition was different at the two positions. The upper photograph in figure 25(b) is a ×1000 magnification of particle 2. It is spherical in shape and from the analysis it consisted of 70-percent aluminum. It was concluded that this particle was aluminum oxide from the rocket exhaust. Particle 3 is shown in the bottom photograph of figure 25(b) with ×1000 magnification. The analysis as shown in table VIII indicates that the particle is mostly sodium chloride as was suspected from the cubical shape.

Delta Gaseous Specie Results

Gas grab samples at all locations showed CO concentrations to be below 2 ppm (limits of detection of analysis). (See appendix B.) Bubblers at sites O, Q, R, S, and 1808 showed no evidence of HCl from the launch (200 ppm/sec detection limit). The bubbler at site MAML did not sample because of power failure. The microcoulometers and M-S-A Billion-Aire analyzer at sites MAML, R, S, and 1808 indicated no HCl (qualitative detection limit of 2 ppm). Values of pH ranged from 1 in the immediate vicinity of the launch vehicle to 3 at a distance of 5 km from the launch vehicle. The pH values of 3 minus (3 -, fig. 26) indicate that the color changes of these papers were slightly less than the pH 3 papers. The pH paper at site S (3 km downwind) was deployed in a roofed tower and thus, possibly accounted for the "no change" indication. In summary, the HCl measurements indicated the presence of HCl at ground level as far as 5 km from the pad, but at concentrations and dosages below 2 ppm and 200 ppm/seconds (detection limits of measurement systems). In addition, the pH paper results indicate that the cloud movement was most likely at a heading of 180^{o} to 270^{o} from the pad.

The results from the gaseous airborne sampling were also qualitative. The HCl measurements (pH paper and mass spectrometer) were qualitative as expected. However, CO results also proved to be qualitative as the duration of the aircraft in the cloud (10 seconds) was considerably less than the response time of the CO detection system (50 to 60 seconds). The infrared CO detector used in the aircraft had a theoretical detection limit of 0.2 ppm, an accuracy of ±0.2 ppm, and a response time including aircraft inlet system of 50 to 60 seconds for 90 percent of full-scale reading. However, in-flight calibration of the CO detector and flow system showed a detection limit of about 2 ppm. Actual CO values are expected to be higher than those measured. Estimation of the actual CO concentrations using the measured values is not practical. Besides the response problem, additional problems were encountered, because of the night launch, of adequately identifying the location of the sampling aircraft with respect to the ground and with respect to the visible cloud. The following is part of the flight log. Three cloud penetrations were documented.

First penetration.- Cloud penetration at T + 3:22 at an altitude of 396 meters. The CO detector indicated 18 ppm maximum, the mass spectrometer indicated 10 ppm HCl, and the pH paper registered a pH of 1.

Second penetration.- Cloud penetration at T + 5:10 at an altitude of 701 meters. The CO detector indicated 10 ppm maximum, the mass spectrometer indicated presence of HCl but less than 10 ppm, and the pH paper measurement malfunctioned.

Third penetration.- Cloud penetration at T + 14:25 at an altitude of 914 meters. The CO detector indicated 2 ppm maximum, the mass spectrometer indicated no HCl, and the pH paper malfunctioned.

Besides these three visible cloud penetrations, additional sampling runs were flown at an altitude of 183 meters along a heading of 215° (predicted cloud path) from the pad. These runs started at the pad and terminated approximately 7 to 8 km from the pad. These sampling runs occurred as early as T + 9 minutes and as late as T + 33 minutes. No CO or HCl above the detection limits of the equipment was noted.

In summarizing the airborne results, it is concluded that HCl and CO were detected in the cloud at levels of approximately 10 ppm and 20 ppm, respectively, that these HCl and CO concentrations are only qualitative and most likely low, and that the night launch made it impossible to identify the aircraft sampling location or the part of the cloud being sampled.

CONCLUDING REMARKS

The preliminary field-monitoring experiments of the two rocket launches served to establish techniques, procedures, and necessary instrumentation requirements for more comprehensive experiments in the future. The exhaust cloud particulate size number distribution (total number of particles against particle diameter), mass loading, morphology, and elemental composition have been determined within limitations. The gaseous species in the exhaust cloud have been identified. The limitations of a few available measuring techniques have been established:

1. Suitable dilution systems should be employed to avoid coincidence problems with the light-scattering photometers. Real-time measurements of particle size number distributions using the light-scattering photometers should be expanded to include the larger particles, greater than 6 μm.

2. Improved laboratory analysis techniques for particulate identification in the lower atomic numbers (less than 10) should be pursued. The X-ray fluorescence, proton scattering, and electron spectroscopy for chemical analysis (ESCA) techniques will be employed in future experiments for elemental analysis.

3. Further improvements in the instrument response times are needed for the airborne measurements of the stabilized ground cloud. Real-time in situ measurements are needed to determine the particulate and gaseous distribution in the cloud.

4. The M-S-A Billion-Aire analyzers and microcoulometer instruments did not provide satisfactory measurements of HCl. Modified sampling techniques and other instruments will be investigated to identify an acceptable real-time HCl detection system.

Langley Research Center,
National Aeronautics and Space Administration,
Hampton, Va., March 7, 1974.

APPENDIX A

PARTICLE MEASURING SYSTEMS

The particulate sampling instrumentation used for monitoring the Scout and Delta launches are listed in table IX.

The Royco Light-Scattering Photometer

The Royco optical system is shown pictorially in figure 27 (from ref. 4). The aerosol or particle to be measured is drawn in at the intake and passes through the illuminated view volume. The right-angle (90^{o}) light scattered by the particle is focused onto a photomultiplier by the lens-slit configuration. The photomultiplier then yields a current pulse proportional to the size particle occupying the view volume at that instant. The particle size range of the instrument is 0.5 μm diameter to 6.5 μm diameter; this size range is divided into 100 channels by a pulse height analyzer (PHA). The PHA provides a size number distribution with printout on paper tape and magnetic tape recording.

The Climet Light-Scattering Photometer

The Climet light-scattering instrument is shown pictorially in figure 28. As with the Royco the aerosol or particle is drawn into the view volume by a vane-type pump which provides a constant airflow rate through the view volume. In addition, the Climet flow system has filtered purge air flowing through the view volume to retain the particles in the center and prevent them from drifting back into the view volume. The light scattered in the forward direction by the particle is focused by the elliptical mirror onto the photomultiplier, the unscattered light passing through the view volume is absorbed by the cone. The photomultiplier output current pulse is proportional to the size of the particle in the view volume. The Climet divides the particles into six size ranges, five ranges from 0.3 μm to 10 μm and the sixth range is 10 μm and greater. The number of particles in the six size range (channels) are printed out on a paper tape to yield number of particles per size range. Since the flow rate (Royco, 0.00005 m^3/sec (0.1 ft^3/min) and Climet, 0.00012 m^3/sec (0.25 ft^3/min)) and sampling time are known for these instruments, the size distribution and number of particles per cubic meter can be determined.

The Quartz Crystal Microbalance (Mass Monitor)

The quartz crystal microbalance (fig. 29) is in effect an impactor in which the particulates impact on a quartz crystal. A sample airflow and electrical schematic is shown in figure 30. The sample is drawn into the instrument by the blower and impacted

on the sensing crystal. The second crystal which is located just behind the sensing crystal serves as a temperature compensator and also as the reference crystal. The sensing crystal is part of a resonant circuit whose frequency is controlled by the resonant frequency of the crystal. As particles impact on the crystal, the crystal is deformed in the shear mode and its frequency is changed. The sensing frequency change is compared in the mixer with the reference frequency, which is 1 to 2 kHz higher, and as the mass is accumulated on the sensing crystal, the beat frequency increases. This beat frequency change is converted to an analog voltage, the derivative of which is proportional to the mass concentration. The saturation output level of 0 to 1 V yields the total mass of particulates in μg accumulated over the sampling period. The concentration output level of 0 to 1 V yields the average (averaged over several seconds) particulate mass concentration in $\mu g/m^3$. The particle-size range of the mass monitor is on the order of 0.1 μm to 100 μm. The 0 to 1 V outputs are recorded on a two-pin strip chart recorder in real time. In addition, the crystals can be removed from the mass monitor and an analysis for elemental and pictorial identification performed on the collected particles by using scanning electron microscope (SEM) techniques.

The Andersen Impactor

The Andersen impactor (fig. 31) is an eight-stage cascade impactor which collects and sizes particulates according to their aerodynamic dimension. The instrument operates as follows (fig. 32): Each of the eight stages has a steel plate with 400 holes in it, the holes decrease in size for each succeeding stage but all the holes in a given stage have the same size. The particles are drawn into the impactor inlet by a separate small vacuum pump at a flow rate of 0.0005 m^3/sec (1 ft^3/min) and drawn through the 400 relatively large holes of the first stage. The velocity of the sample is increased by its flow through the holes, the particles depending on their aerodynamic dimension, are either impacted on the collection surface located 2.5 mm below the stage or are carried to the edge of the first-stage plate by the airstream and on to the second stage. By measuring the number of particles collected and applying the appropriate collection efficiency factor (see fig. 33 which is from ref. 5), one can calculate the number of particles of a given size. The process is repeated in the second stage which has smaller holes and thus increased velocity and this process is repeated in each succeeding stage (each stage having progressingly smaller holes and producing greater increases in velocity) until the particles are captured in one of the stages. The collection surfaces can be glass, steel, Nuclepore or cellulose acetate filter paper, and so forth, depending on the requirements of the particular sampling application. The impactor collects particles in seven size ranges from 0.43 μm to 11 μm plus the first stage which collects particles above 11 μm. The substrates can be analyzed by gravimetric, particle counting, neutron activation, and so forth, to yield information on mass, size distribution, elemental content, and so forth.

High-Volume Samplers

The high-volume samplers are shown in figure 34 without housing. The units are essentially high flow rate motors with various configurations for holding the sampling filters. They can be packaged in different types of shelters for weather protection and long-term sampling. Depending on the type of sample and filter material, the sampling rate will be in the range of 0.019 to 0.038 m^3/sec (40 to 80 ft^3/min). For the single-stage units, the filters are usually 20.3 by 25.4 cm (8 by 10 in.) in size or 10.16 to 15.24 cm (4 to 6 in.) in diameter. Filter material can be one of several different types such as fiberglass, cellulose, cellulose-asbestos, cellulose-glass, and polystyrene. In operation, the filter is placed in the head and clamped in place. The motor is started and the particles are drawn toward the filter surface and are collected by direct interception and inertial collection. The sampler on the left in figure 34 has an Andersen sizing head attached. This configuration yields aerodynamic sizing of particulates into five size ranges from 0.01 to 7.0 μm. In this configuration, the flow rate is 0.0094 m^3/sec (20 ft^3/min). Collection is on substrates such as Nuclepore, cellulose, aluminum, and others. After collection of the particulates, the filters can be analyzed by gravimetric, neutron activation analysis, and other techniques to yield information on mass, size distribution, and elemental content. Since the flow rate and sample time are known, the average mass per volume ($\mu g/m^3$) can be determined.

Two types of membrane filter holders are shown in figure 35. The millipore holder shown accepts 37-mm-diameter filters, and the Nuclepore holder accepts 47-mm-diameter filters. Membrane filters are made in many different materials such as cellulose, nylon, teflon, silver, and polycarbonate. To collect samples with a membrane filter, the filter is placed in a holder (fig. 36) and clamped in place by various retaining ring configurations. A vacuum pump is attached to the suction tube and turned on, the resulting flow rates of 0.00009 to 0.0024 m^3/sec (0.2 to 5 ft^3/min) depending on filter material, pore size, pump capacity, and so forth. The particles are drawn by the vacuum pump induced flow to the filter surface and collected primarily by diffusion and impaction with electrostatic forces playing a small part. For samples to be run for relatively long periods of time, a flow-limiting orifice can be placed in the suction tube to keep the flow relatively constant. After the particulates are collected, the filters can be subjected to all the analysis techniques mentioned previously and, in addition, can have particle counting performed by systems such as the particle measuring computer (designated πMC). In addition, several different pore size filters can be used to perform simultaneous sampling and thus yield size distributions of the particulates.

The Lundgren Impactor

The Lundgren impactor is shown in figure 37. The Lundgren impactor has four stages with each stage having a rotating drum as shown. The size ranges as determined by the 50-percent cut points are 14 μm diameter for stage 1, 3.8 μm for stage 2, 1.1 μm for stage 3, and 0.5 μm for stage 4. The substrate on the rotating drum can be coated with a grease, the type of grease depending on sampling conditions. Substrates such as Mylar, Teflon, and Nuclepore can be used for particle collection. The rotation speed of the drums can be varied to obtain a real-time distribution of particulates collected over various time periods for the four size ranges. A suitable vacuum pump is coupled to the instrument through a final filter and provides up to 0.0024 m^3/sec (5 ft^3/min) airflow through the instrument. The particles enter the first stage through a slit and those having enough inertia follow the air streamlines around the first drum to the second slit and the process is repeated with the final filter on the outlet of the instrument collecting all particles not collected on the four rotating drum stages. The substrates can be weighed for total particulates collected or can, depending on accumulation, have particle counting performed on them. Elemental analysis can be performed on the uncoated substrates utilizing the other previously mentioned analysis techniques.

APPENDIX B

GASEOUS MEASURING SYSTEMS

pH Sensitive Paper (HCl)

Certain natural and synthetic colored substances (for example, methyl orange and methyl red) have the property of changing color when the hydrogen ion concentration in the solution attains a certain value. A great number of such substances are known and careful blending of these substances can produce indicators which are sensitive to a wide range of hydrogen ion concentration (pH = 0 to 14) and which are capable of defining pH to within a 1/2 pH unit. The pH papers used for the Scout and Delta launches were commercially available papers selected to cover the pH range of 1 to 7 in increments of 1 pH units. Theoretically, in the presence of ambient moisture (greater than 50-percent relative humidity), the color change of a paper can be related to HCl exposure (concentration times time) by laboratory calibration. However, results in this laboratory have not shown the color changes of the papers to be quantitatively related to HCl exposure. Instead, the laboratory results have shown the color change of the papers to fall into one of three classes of response: (1) A discrete color change defined as pH = 1 by the manufacturer, (2) a discrete color change defined as pH = 3 by the manufacturer, and (3) a partial color change or spotting of the paper, not defined by the manufacturer. (For purposes of discussion these classes will be referred to as pH = 1, pH = 3, and "acid indication.") These three classes of response permit the papers to be used as a qualitative indicator of the presence of HCl as verified by the following laboratory and field observations.

1. Tests conducted in the laboratory at HCl concentrations ranging from 0.5 ppm to 20 ppm and for exposure times ranging from a few seconds to several minutes resulted in three types of pH paper color changes: for a given HCl concentration, increasing the exposure time resulted in the papers progressing from a no acid color (original color), to an "acid indication," to a pH = 3 indication, and then to pH = 1 indication.

2. The pH = 3 and pH = 1 indications occur only after certain acid exposure of the papers. Routine ambient monitoring with the pH paper produced no color changes in the pH = 3 or pH = 1 class.

3. Papers classed above as "acid indication" were found to be unreliable. In addition to the spotting (difficult to interpret) type color response, a similar type of color response could sometimes be obtained during routine ambient monitoring. It is not known whether during these ambient measurements the environment did indeed have some acid present.

4. Color changes associated with "acid indication" responses were temporary and reverted to the original color (no acid indication) within 2 to 3 hours; whereas, the color changes associated with pH = 3 and pH = 1 were retained for several days and

indefinitely if sealed in plastic bags within a day of having been exposed. All pH papers exposed during the Scout and Delta launches were retrieved and sealed in plastic bags within 2 to 3 hours after launch.

As a result of these laboratory studies, only the color changes associated with pH = 3 and pH = 1 are considered to be valid indicators of HCl from the launch vehicles, and then only qualitatively identifying those areas receiving more HCl exposure than other areas.

Whole Air Grab Samplers (CO)

Two types of grab samplers were used. For the Scout launch, 500 cm^3 stainless-steel cylinders of the type shown in figure 38 were used. Each cylinder was equipped with a pump-out valve for evacuation of the sampler prior to launch, a vacuum gage for monitoring the vacuum level in the evacuated cylinder, and an electrically operated solenoid valve for venting the sampler to atmospheric pressure with the launch sample. Each sampler was vacuum baked (24 hours at 200° C and 1×10^{-5} N/m^2) and then evacuated to approximately 6 N/m^2 (5×10^{-2} torr) approximately 1 week prior to launch. Appropriate background analysis and pressure checks were performed to insure that each sampler maintained its vacuum and cleanliness up to launch. Each sampler was vented to atmosphere by a preprogramed electrical signal from the launch computer. Vent time from the evacuated state to atmospheric pressure was approximately 3 seconds.

The whole air samplers for the Delta launch were 35-liter stainless-steel containers. They were equipped with only a pump-out valve which was used for evacuation as well as for sampling. Samplers were manually vented on a schedule based on real-time observation (particulate measurements) of cloud presence or a preprogramed schedule based on predicted cloud behavior.

As stated in the text, the Scout and Delta whole air samples were valid only for CO detection. The limit of detection for Scout was 0.1 ppm (±0.1 ppm or 10 percent accuracy, whichever is largest); for Delta, 2 ppm (±10 percent accuracy). The difference in the detection limits is attributed to the different sampling containers as well as to the analysis techniques used.

Microcoulometer Sampling System (Chlorides)

The microcoulometer sampling systems used during the Delta launch are shown schematically in figure 39. Each system consists of a coulometer and a titration cell, an air sampling pump (200 to 300 cm^3/min), and an appropriate data recording system. The system detects the chloride present in the HCl and operates on null-balance microcoulometric principles. The titration cell is composed of four electrodes of which two function as a sensing pair while another pair functions as a generating (titration) pair. The cell

electrolyte is basically 70 percent acetic acid with a silver ion concentration of approximately 10^{-7} mole/liter. The cell electrolyte is continually stirred (magnetic stirrer) and maintained at the silver ion concentration by appropriate bias settings on the electrodes. Chloride upon entering the cell reacts with silver ions and results in a decrease in the silver ion concentration. This silver ion concentration change is immediately sensed by the sensor electrodes in the form of a voltage change. Through appropriate circuits this voltage change supplies power to the generating electrodes, which, in turn, deplate silver to reestablish the initial silver ion concentration in the cell. The current passing between the generating electrodes is measured and this quantity of electrical energy is directly related, by Faraday's Law, to the amount of silver required to return (null) the cell to its original concentration.

The microcoulometer has a real-time lower detection limit of 3 nanograms of chloride (not considering inlet HCl reactions). It is estimated, based on current laboratory investigations, that the microcoulometer measurement system used in the Delta launch would respond in real time and quantitatively to a 20-second duration of HCl at a level of 2 ppm.

Billion-Aire Sampling System (HCl)

The Billion-Aire sampling systems used during the Delta launch were the portable units manufactured by Mine Safety Appliances Company. The unit was set up for acid detection and used amine reagent to react with the incoming sample. Basically, the Billion-Aire analyzer uses an ionization chamber to detect an aerosol which is formed by reacting the incoming HCl sample with the amine reagent. Prelaunch laboratory calibration of the Billion-Aire system with dry N_2-HCl mixtures showed a qualitative response to HCl at the 2 ppm level in approximately 10 seconds; however, several minutes were required to quantitize at the 2 ppm level.

Bubbler Sampling System (Chloride)

The bubbler sampling system consisted of a fritted bubbler and pump as shown in figure 40. Flow rate for each bubbler was 2832 cm^3/min (0.1 ft^3/min) and was controlled by a bleed valve on the inlet of the pump. The bubbler fluid was distilled water. Analysis of the bubbler fluid was for chloride using coulometric techniques. As discussed in the test, the bubbler system had a lower detection limit of approximately 200 ppm/sec.

APPENDIX C

PARTICULATE ELEMENTAL ANALYSIS TECHNIQUES

The methods now being used or being considered for use for elemental analysis are as follows: (1) X-ray fluorescence, (2) X-ray analysis, (3) proton scattering, (4) neutron activation, (5) atomic absorption, and (6) electron spectroscopy for chemical analysis (ESCA). A brief description of the techniques is given in this appendix.

X-Ray Fluorescence

This technique allows the elements of a collected sample to be identified from the energy spectrum of X-rays emitted when the sample is exposed to a beam of X-rays. The electrons are removed from the inner shells of the atoms by the beam. The outer shell electrons move in to fill the vacancies and X-rays are emitted in the process. The energies of the X-rays are characteristic of the particular elements involved. Thus, if the X-ray energy spectrum is measured, the elements present in the sample can be identified. Elements with atomic numbers less than 12 are not detected by this method because the energies of the emitted X-rays are too low to penetrate the windows of commonly available detectors.

X-Ray Analysis

The principle of X-ray analysis is the same as that for X-ray fluorescence in that characteristic X-rays are emitted from the atoms in the same manner. (See refs. 6 and 7.) The primary difference between the two techniques is that electrons are used to induce X-ray emission with X-ray analysis instead of X-rays. Usually this technique employs the scanning electron microscope, both as an electron source and as an analyzer. Elements with atomic numbers less than 11 are not detected with this method.

Proton Scattering (Elastic Scattering)

In the proton scattering technique the sample is exposed to a beam of protons of a given incident energy E_{inc}. An elastic scattering takes place between the atomic nucleus and the proton. The scattered proton suffers an energy loss ΔE.

$$\Delta E = E_{inc} - E_{sc}$$

From elastic scattering calculations at 90^{o} for simplicity, it can be shown that

$$\Delta E = \frac{2E_{inc}}{(1 + A/a)}$$

where

A mass of target nucleus

a mass of proton

The loss ΔE is determined by measuring the scattered energy E_{sc}. (See ref. 8.) Then from this equation, A is calculated. Since A is the atomic mass, the element is readily determined. It can be seen from the equation that for small values of A, unit changes in A give large changes in ΔE. Therefore, the sensitivity of this technique increases as the atomic mass decreases. Hence, hydrogen with an atomic number of 1 can be detected.

Neutron Activation Analysis

The sample is exposed to a beam of neutrons which enter the nucleus of the atom. The atom then becomes radioactive and emits radiation as it decays. The gamma radiation is measured and analyzed. From the energy spectrum of the radiation, the elements present in the sample are determined.

Atomic Absorption

In the atomic absorption technique the sample is dissolved by chemicals and properly diluted. The spectral absorption is then measured with a spectrophotometer. The absorption spectra is characteristic of the chemical elements present in the material.

Electron Spectroscopy for Chemical Analysis (ESCA)

Electron spectroscopy for chemical analysis (ESCA) gives both elemental composition and chemical coordination of a material. The sample is exposed to a beam of high-energy X-rays which interact with electrons in the inner and outer atomic shells. The electrons are ejected with energies E_k given by

$$E_k = h\nu - E_n$$

where $h\nu$ is the photon energy and E_n is the chemical binding energy. By measuring the kinetic energy of the photoelectrons, the binding energy can be calculated. This value can then be compared with a table of binding energies based on elemental standards to determine the elements present.

Of these methods for elemental analysis, X-ray fluorescence, X-ray analysis, neutron activation, and atomic absorption were used to analyze materials collected during

the two launches discussed in this report. Proton scattering and ESCA were not used. The results from preliminary studies utilizing the proton scattering and ESCA techniques look promising and will be used in subsequent analysis.

REFERENCES

1. Stephens, J. Briscoe; Susko, Michael; Kaufman, John W.; and Hill C. Kelly: An Analysis of the Dispersion Predictions for Effluents From the Saturn V and Scout-Algol III Rocket Exhausts. NASA TM X-2935, 1973.

2. Kaufman, John W.; Susko, Michael; and Hill, C. Kelly: Prediction of Engine Exhaust Concentrations Downwind From the Delta-Thor Telsat-A Launch of November 9, 1972. NASA TM X-2939, 1973.

3. Chuan, Raymond L.: An Instrument for the Direct Measurement of Particulate Mass. Aerosol Sci., vol. 1, no. 2, May 1970, pp. 111-114.

4. Morse, F. L., Jr.: The Aerosol Particle-Size Distribution Measuring System. Aerospace Rep. No. ATR-70(8103)-1, Aerospace Corp., Feb. 1, 1970.

5. Anon.: Air Sampling Instruments for Evaluation of Atmospheric Contaminants. Fourth ed., American Conference Governmental Industrial Hygienists, c.1972.

6. McCrone, Walter C.; and Delly, John Gustav: The Particle Atlas. Vol. II – The Light Microscopy Atlas. Second ed., Ann Arbor Sci. Publ., Inc., c.1973.

7. Johansson, T. B.; Akelsson, R.; and Johansson, S. A. E.: X-Ray Analysis: Elemental Trace Analysis at the 10^{-12}g Level. Nuclear Instruments & Methods, vol. 84, 1970, pp. 141-143.

8. Jolly, R. K.; and White, H. B., Jr.: Elemental Analysis by Elastic Scattering. Nuclear Instruments & Methods, vol. 97, no. 2, Dec. 1971, pp. 299-307.

TABLE I.- SCOUT LAUNCH PARTICULATE MONITORING SITES

Site number	Angle from launch point, deg	Distance from launch point, m	Remarks
1	350	62.5	Top of NASA van, ≈4.6 m
3	38	117.3	Roof of building W-125, ≈3.7 m
4	135	76.8	Top of 6.1 m tower
5	225	99.4	Top of 6.1 m tower
6	270	94.2	Top of 6.1 m tower
7	293	23.2	Roof of building W-100, ≈6.1 m
8	333	129.2	Roof of building W-65, ≈10.7
9	335	254.8	Top of 6.1 m tower
10	183	68.6	Top of NASA van, ≈4.6 m
11	22	376.7	Top of 3.7 m tower
12	24	533.4	Top of 9.1 m tower

TABLE II.- HIGH-VOLUME MEASURED AEROSOL MASS LOADING DATA

Day in Aug. 1972	Mass loading, $\mu g/cm^3$, at –			
	Site 4	Site 7	Site 8	Site 9
10	58		27	
[a] 10-11			31	
[a] 11-12		61	27	
12	43	59		
[a] 12-13				47
13 (launch day)	115 [b] (20 min)	1851 [b] (9 min)	187 [b] (19 min)	162 [b] (15 min)
14		58		
[a] 14-15			67	
15		42		

[a] Collection on parts of both days.

[b] Collection time during launch.

TABLE III.- ELEMENTAL ANALYSIS OF AEROSOLS BY NEUTRON ACTIVATION

[Values in excess of clean filter in $\mu g/cm^3$; all values ±10 percent]

Element	Analysis at prelaunch at site 3, filter 62	Analysis at launch at –							Analysis at postlaunch at –	
		Site 8, filter 62	Site 3, filter 78	Site 7, filter 84	Site 5, filter 90	Site 6, filter 96	Aircraft, filter 102	Site 1, filter 48	Site 1, filter 114	Site 3, filter 156
Al . . .	2.62×10^{-2}		4.75×10^{-2}	2.43×10^{1}			6.04×10^{-1}	1.01×10^{2}	3.59×10^{-2}	1.04×10^{-1}
Cl . . .	6.03×10^{-1}	2.84×10^{1}	1.23×10^{1}	1.10×10^{2}	3.93×10^{2}	1.60×10^{1}	2.40×10^{1}	8.27×10^{1}	1.45×10^{1}	3.54×10^{1}
Cu . . .		2.51×10^{-1}	1.71×10^{-2}					3.68×10^{1}	3.47×10^{-2}	6.04×10^{-3}
I	2.01×10^{-4}	2.52×10^{-2}	5.70×10^{-3}	4.42×10^{-1}	3.93×10^{-1}	2.24×10^{-1}	1.11×10^{-1}	9.66×10^{-2}	1.66×10^{-4}	1.75×10^{-2}
Mn . . .	6.37×10^{-3}		5.22×10^{-3}			1.28×10^{-1}	3.20×10^{-2}			
Na . . .	1.01×10^{-2}		4.55×10^{-1}			9.60×10^{-1}	3.20×10^{1}		7.02×10^{-1}	5.85×10^{-1}
Mg . . .	6.03×10^{-2}								2.10×10^{-1}	7.39×10^{-1}
Fe . . .	2.42×10^{1}					4.80×10^{2}			9.92×10^{-1}	2.83×10^{1}
Ti . . .									1.57×10^{-1}	

TABLE IV.- CO CONCENTRATION DATA

[Scout launch]

Site	Time sample* initiated					
	T = 0 seconds	T + 5 seconds	T + 10 seconds	T + 15 seconds	T + 30 seconds	T + 60 seconds
1	<0.5 ppm	0.8 ppm	--------	<0.5 ppm	--------	10.5 ppm
3	--------	--------	--------	<0.5 ppm	<0.5 ppm	--------
4	<0.5 ppm	1.0 ppm	<0.5 ppm	<0.5 ppm	--------	<0.5 ppm
7	<0.5 ppm	<0.5 ppm	<0.5 ppm	--------	--------	<0.5 ppm
8	--------	0.8 ppm	--------	2.0 ppm	16.5 ppm	14.8 ppm
10	--------	--------	<0.5 ppm	<0.5 ppm	<0.5 ppm	<0.5 ppm

*In each case the sampling duration was 2 to 3 seconds.

TABLE V.- T-10 HOUR EFFLUENT PREDICTION

[Delta Telsat-A launch]

Ground cloud stabilization altitudes:
- Top of cloud, m 725
- Center of cloud, m 600

Wind velocities:
- Surface from 020°, m/sec 6
- 725 m from 050°, m/sec 5

Predicted cloud parameters:
- Cloud velocity from 035°, m/sec 5.5
- Stabilization altitude (top of cloud), m 725

HCl dosage at altitude of 2 meters:
- 3 km downwind, ppm/sec 17
- 15 km downwind, ppm/sec 64

TABLE VI.- T-3 HOUR EFFLUENT PREDICTION

[Delta Telsat-A launch]

Ground cloud stabilization altitudes:
- Top of cloud, m 850

Wind velocities:
- Surface from 040°, m/sec 3.5
- 850 m from 030°, m/sec 3.0

Predicted cloud parameters:
- Cloud velocity from 035°, m/sec 3.25
- Stabilization altitude (top of cloud), m 850

Downwind distance, km	Surface			Cloud		
	Peak concentration, ppm	Average concentration, ppm	Dosage, ppm/sec	Peak concentration, ppm	Average concentration, ppm	Dosage, ppm/sec
Concentrations of HCl						
1	0.010	0.007	1.8	9.4	5.5	1361
3	.050	.031	7.9	3.6	2.1	545
5	.100	.060	16.8	1.9	1.1	313
10	.160	.093	33.8	.6	.4	132
Concentrations of CO						
1	0.04	0.02	5.4	27.6	16.1	3981
3	.15	.09	23.2	10.6	6.2	1595
5	.30	.18	49.0	5.6	3.3	916
10	.47	.27	98.9	1.8	1.1	385

TABLE VII.- CLOUD ARRIVAL AND PASSAGE TIME FOR GROUND SITES

Cloud arrival time: time after launch at which cloud was predicted to have passed a given location

Cloud passage time: time after launch at which cloud was predicted to have passed a given location

Downwind distance, km	Cloud arrival time, min after launch	Cloud passage time, min after launch
1	3.1	7.2
3	13.2	17.5
5	23.3	28.3
10	48.3	54.3

TABLE VIII.- DELTA LAUNCH SEM PARTICULATE ANALYSIS

Element	Particle, relative amounts, percent by weight			
	1-1	1-2	2	3
Na	34.0	23.6		50.3
Al	9.1	14.8	70.7	1.2
Si	11.0	18.0	2.9	.8
Au				
S		15.9		
Cl	38.3	5.6	26.4	47.8
K	4.7	8.6		
Ca	2.8	6.8		
Ti		6.7		

TABLE IX.- PARTICLE SAMPLING INSTRUMENTATION

[Neutron activation analysis, NAA
Particle measuring computer, πMC
Scanning electron microscope, SEM]

Instrument	Type	Number of stages or ranges	Particle size range (diameter), μm	Flow rate, m^3/sec	Filter size	Filter type	Type of data obtained	Data analysis techniques
Royco	Light scattering (right angle)	100 channels	0.5 to 6.5	0.00005			Number of particles; size distribution; and real time	Paper and magnetic tape readout
Climet	Light scattering (forward)	6 channels	0.3 to 0.5; 0.5 to 1.0; 1.0 to 3.0; 3.0 to 5.0; 5 to 10; and >10	0.00012			Number of particles; size distribution; and real time	Paper and magnetic tape readout
Mass monitor	Quartz crystal microbalance	2 stages	0.1 to 100	0.00003			Mass, $\mu g/cm^3$; elemental composition; and real time	Real-time mass readout on strip chart; SEM; and response time <5 sec at concentration of 10 $\mu g/cm^3$
Andersen	Cascade impactor	8 stages	0.43 to 11.0 and >11	0.000472	82 mm	Substrates of Nuclepore, cellulose, glass, and steel	Size distribution; elemental composition; particle count; and mass, $\mu g/cm^3$	πMC; SEM; NAA; gravimetric; and X-ray fluorescence
General Metal Works	High volume with cascade impactor	1 stage + 4 stages	0.01 to 7 and >7	0.00944	20.32 by 25.4 cm + 30.48 cm	Glass fiber	Size distribution; elemental composition; and mass, $\mu g/cm^3$	SEM; NAA; X-ray fluorescence; gravimetric; and chemical
Misco	High volume	1 stage	All above 0.01	0.03304 to 0.03776	20.32 by 25.4 cm	Glass fiber cellulose	Mass, $\mu g/cm^3$ and elemental composition	Gravimetric; SEM; NAA; X-ray fluorescence; and chemical
Nuclepore	Filter media	1 stage	All above 0.1	0.000472 to 0.00094	34 to 47 mm	Nuclepore	Size distribution; mass, $\mu g/cm^3$; particle count; and elemental composition	πMC; SEM; NAA; X-ray fluorescence; gravimetric; and chemical
Lundgren	Inertial impactor	4 stages	50% cut points: 1 to 14; 2 to 3.8; 3 to 1.1; and 4 to 0.5	0.00189	25.4 cm	Nuclepore substrate	Time resolved; size distribution; mass, $\mu g/cm^3$; and particle count	πMC, SEM, NAA, X-ray fluorescence; gravimetric; and chemical

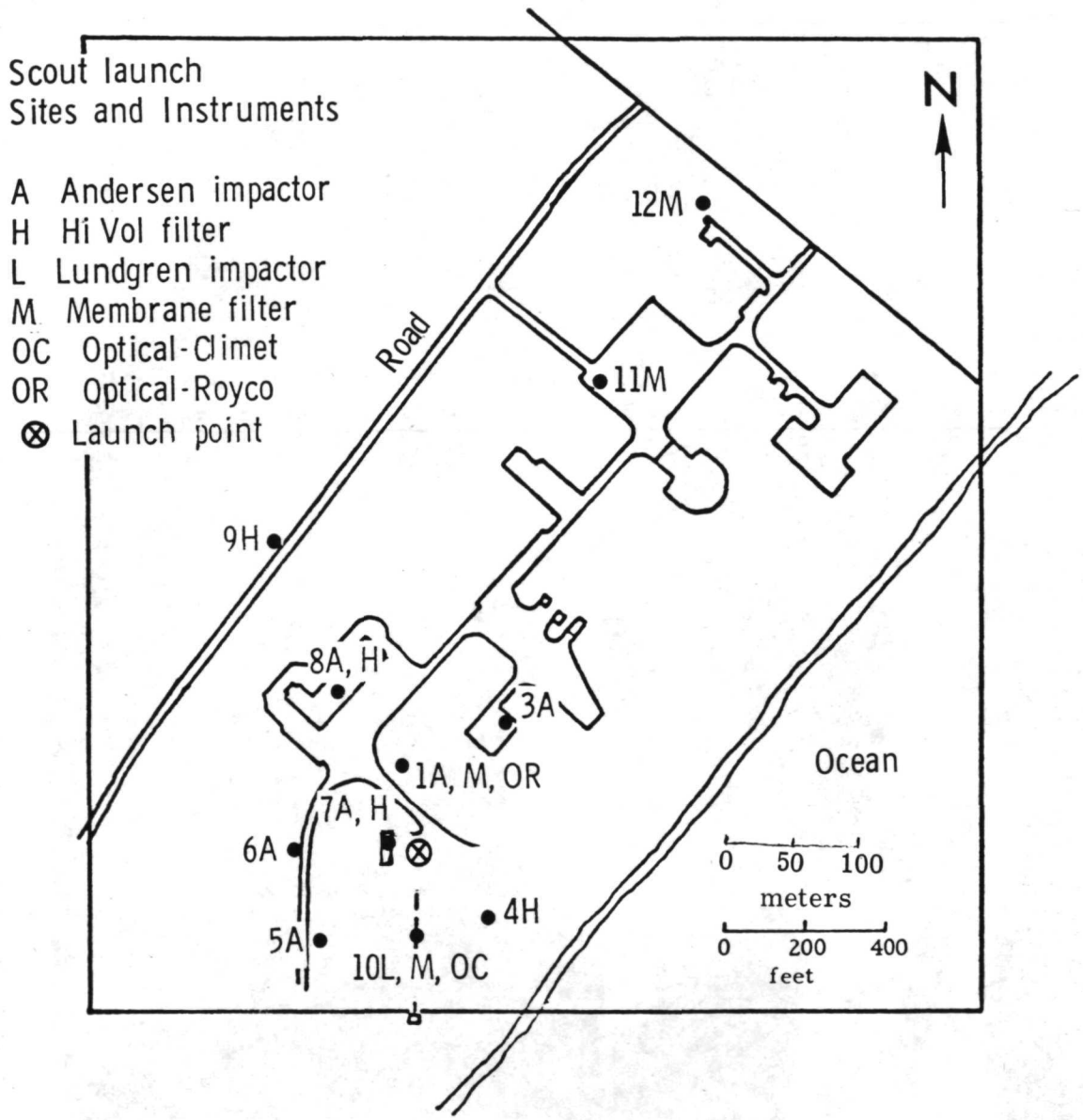

Figure 1.- Map of particulate monitoring instrumentation sites relative to Scout launch point.

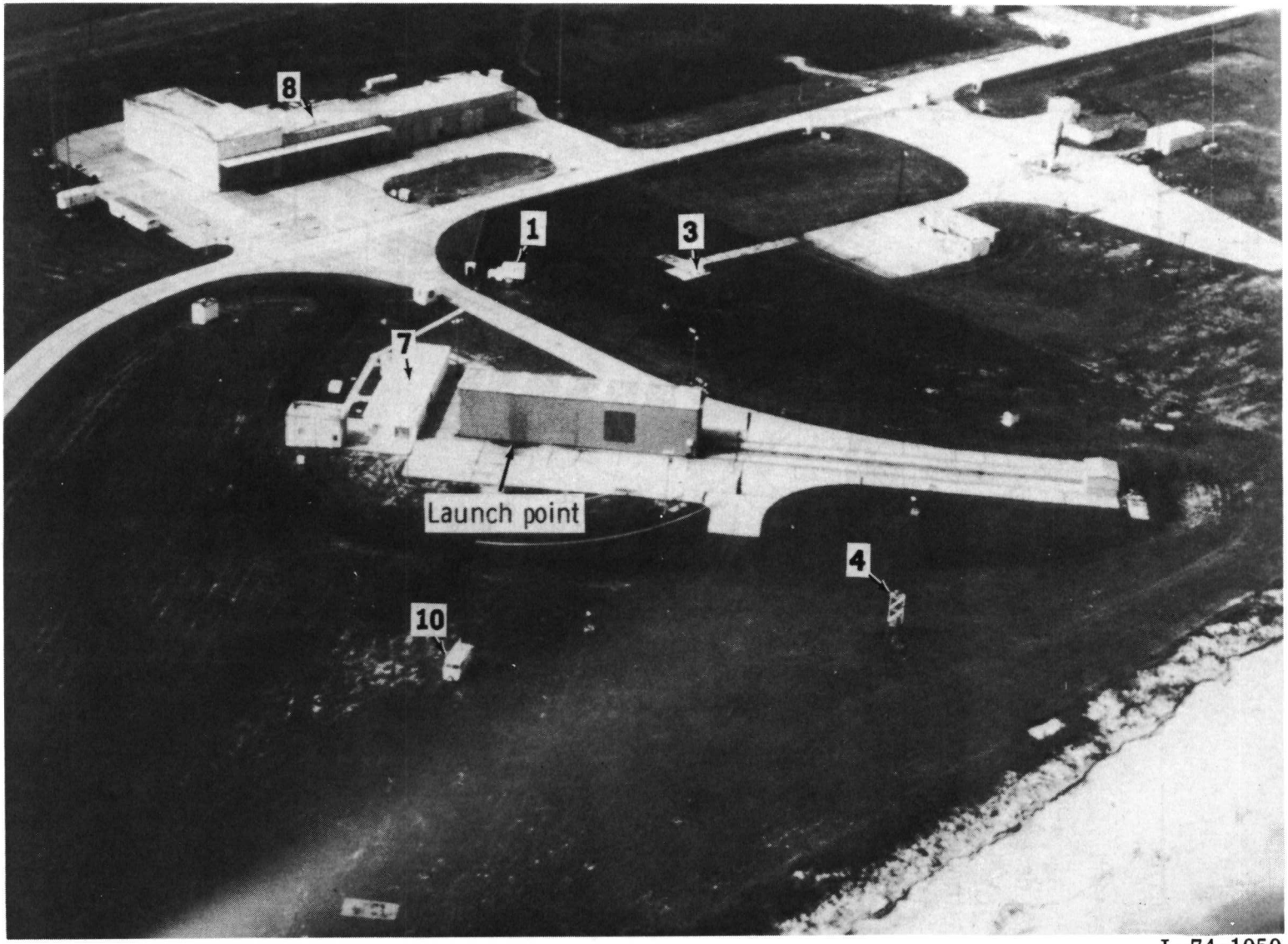

L-74-1050

Figure 2.- Aerial view of Scout launch point and some of the monitoring sites listed in table I.

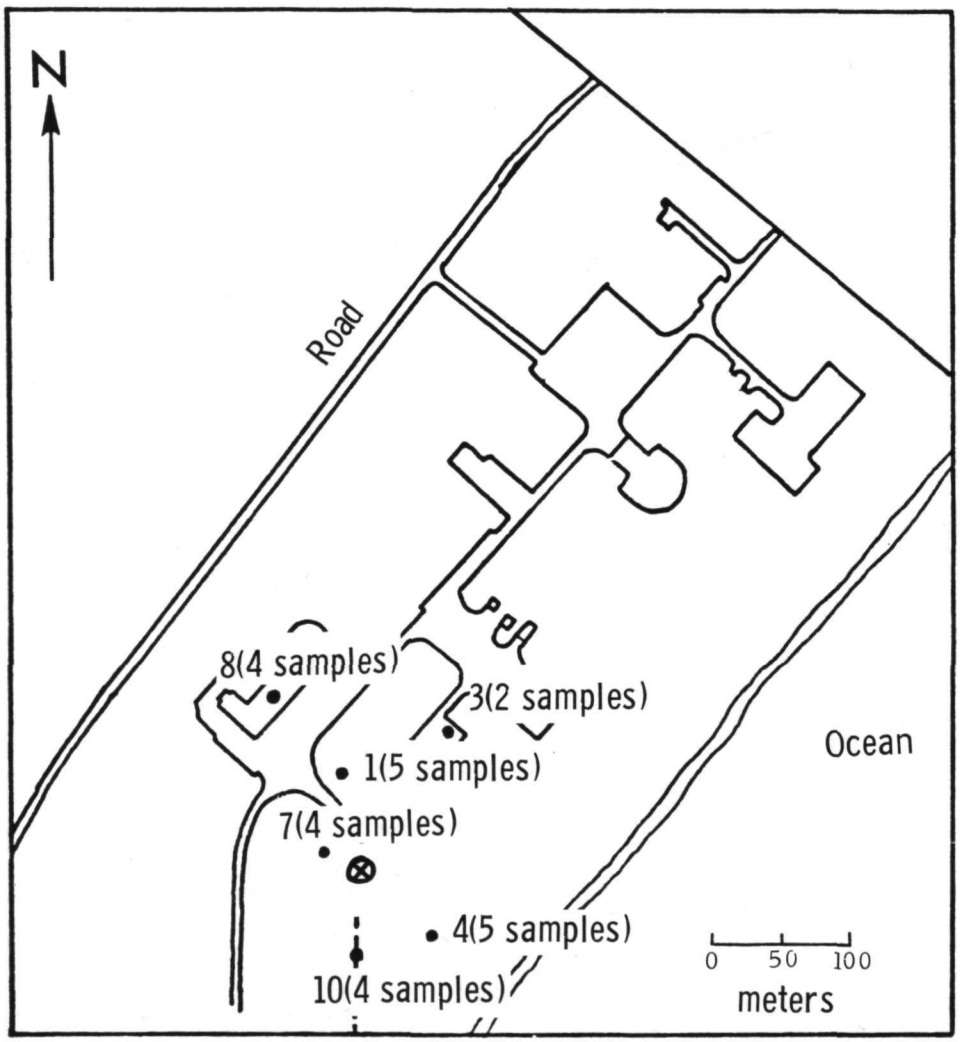

Figure 3.- Map of CO and CO_2 gas grab sampler sites relative to Scout launch point.

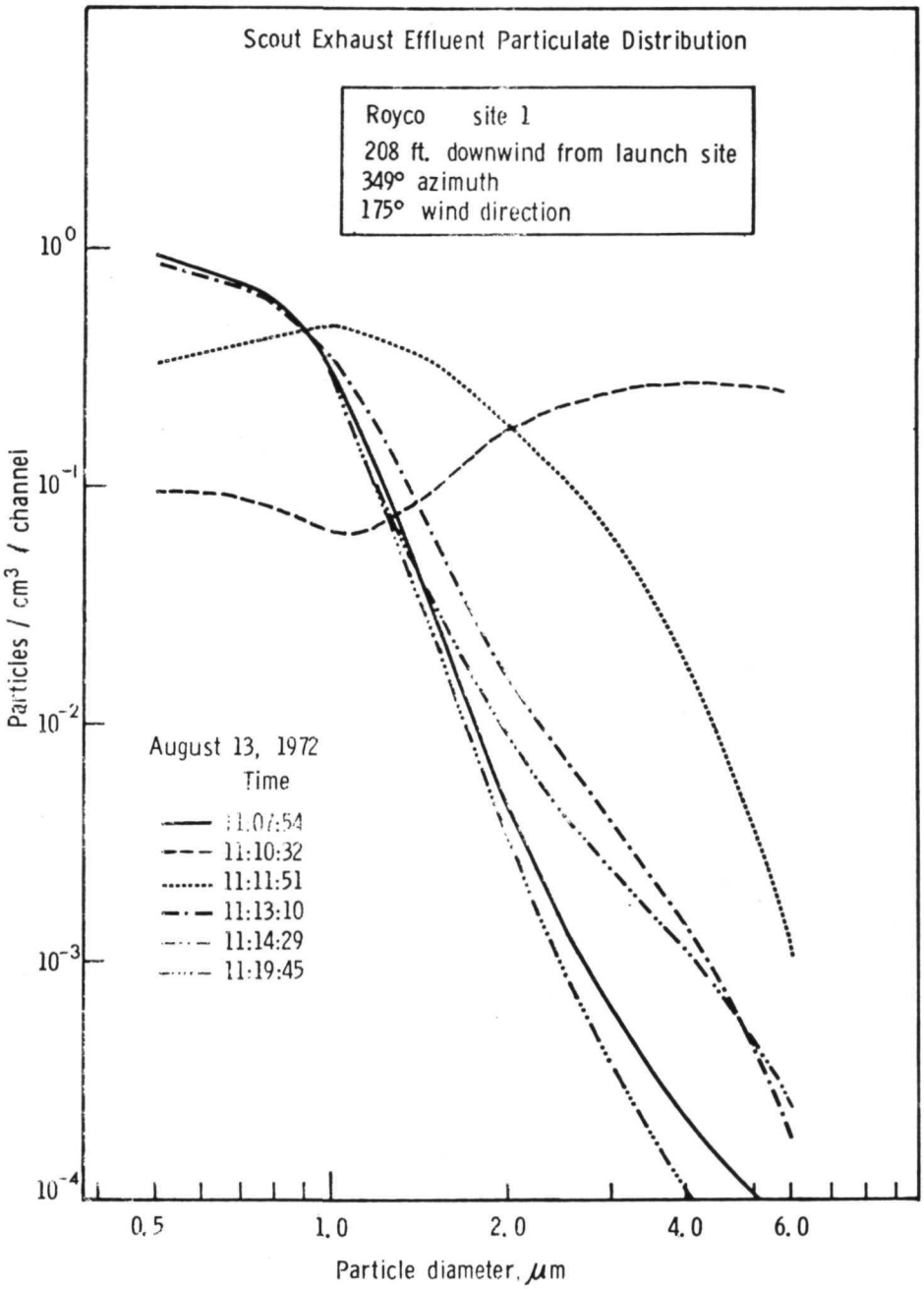

Figure 4.- Particulate size distribution measured at site 1 before, during, and after launch of the Scout rocket.

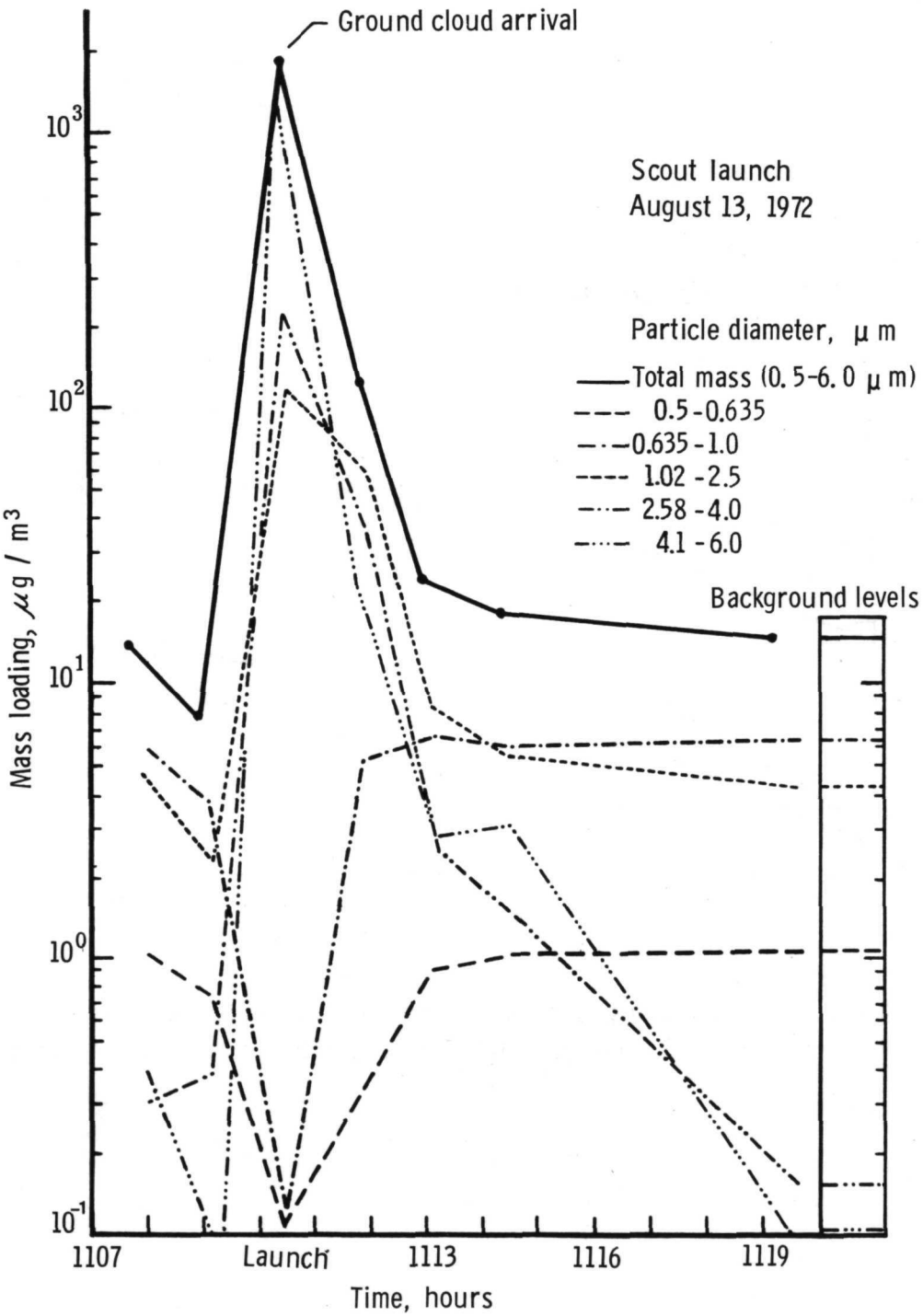

Figure 5.- Particulate mass loading for several size intervals at site 1 before, during, and after launch of the Scout rocket.

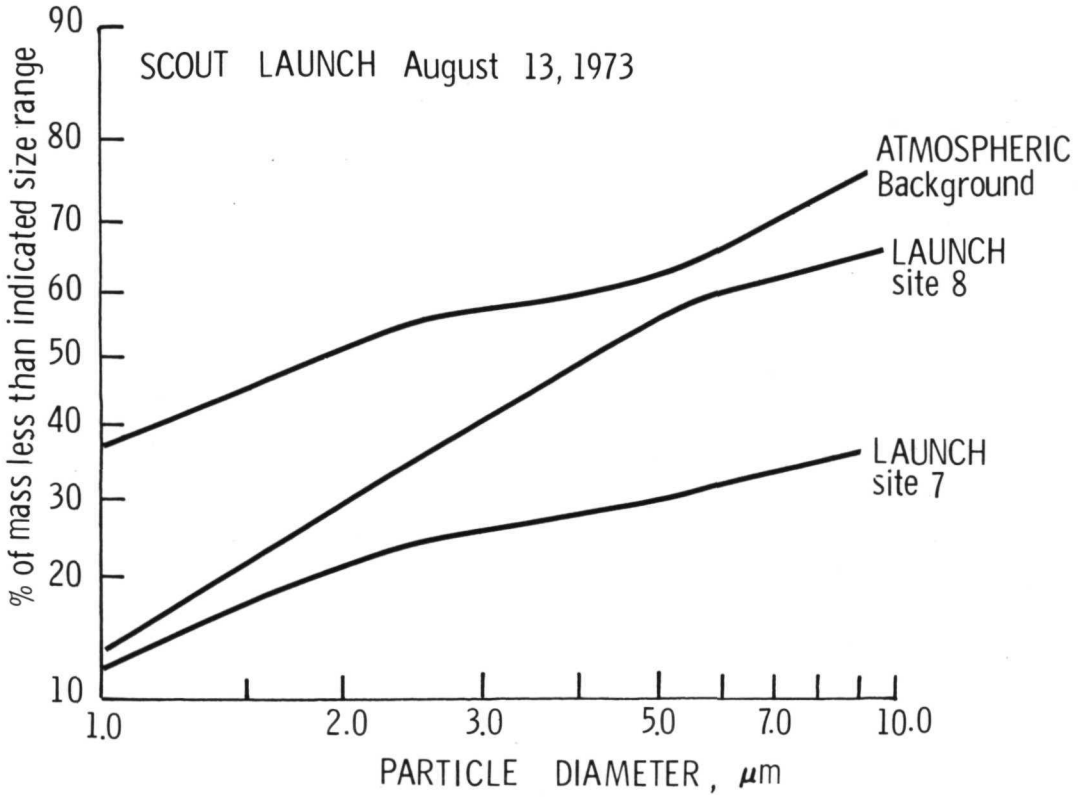

Figure 6.- Log probability plot of particulate mass collected with the Andersen sizing head on the high volume instrument at sites 7 and 8.

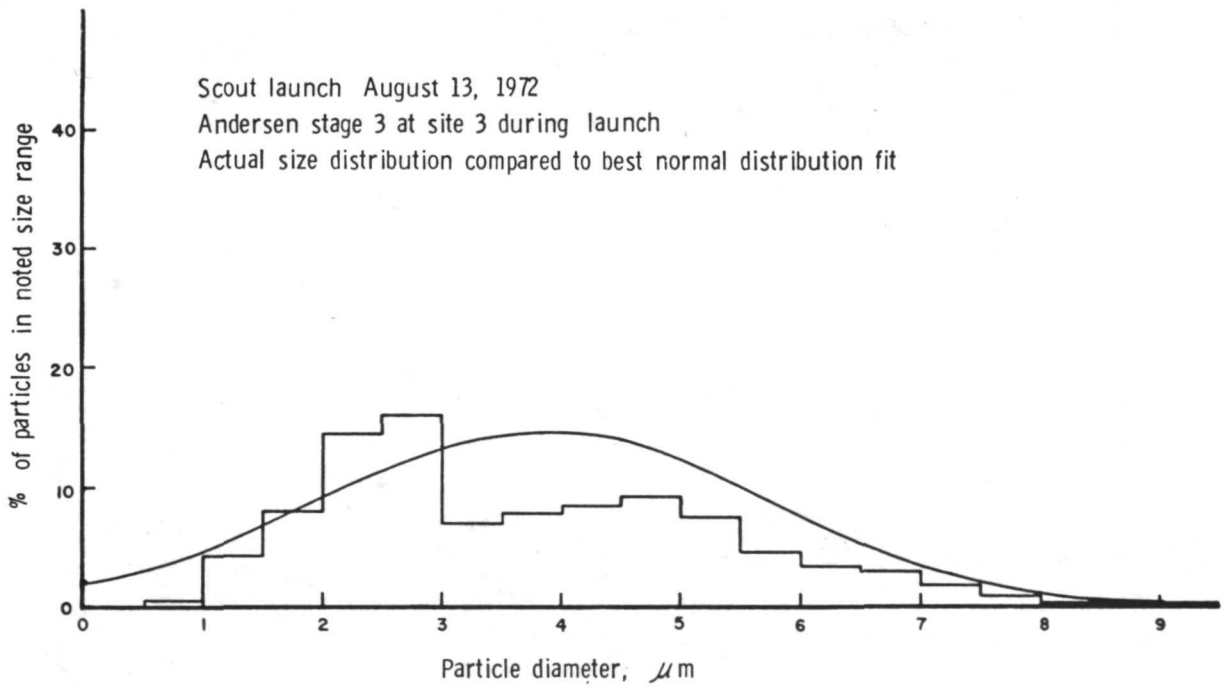

Figure 7.- Particulate frequency distribution plot from the Andersen stage 3 at site 3 measured during launch of the Scout rocket.

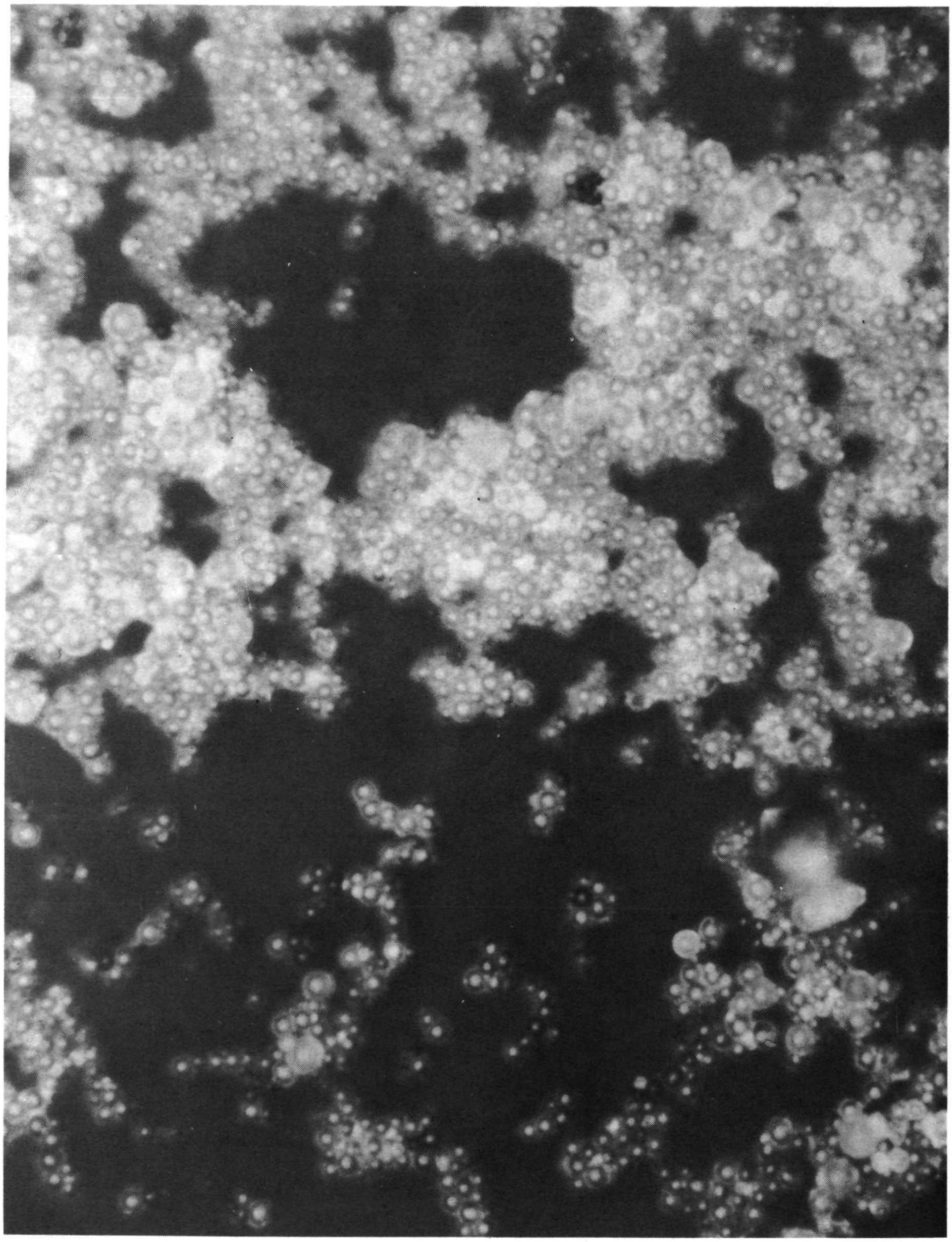

L-74-1051

Figure 8.- Spherical-shaped aluminum particles (×1600 magnification) collected on Andersen stage 3 at site 1 during launch.

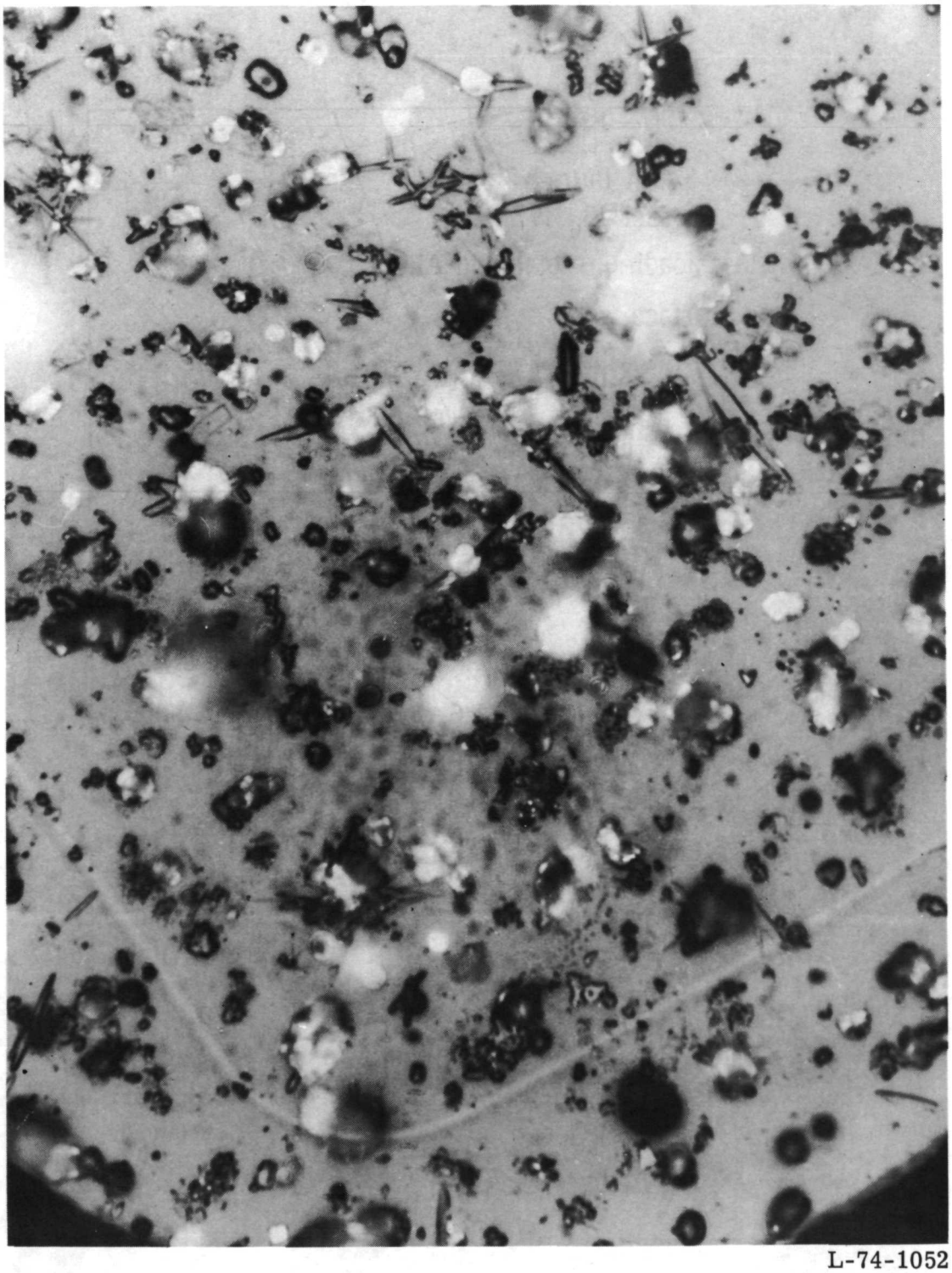

L-74-1052

Figure 9.- Atmospheric background particulates (×1600 magnification) collected on Andersen stage 3 at site 1.

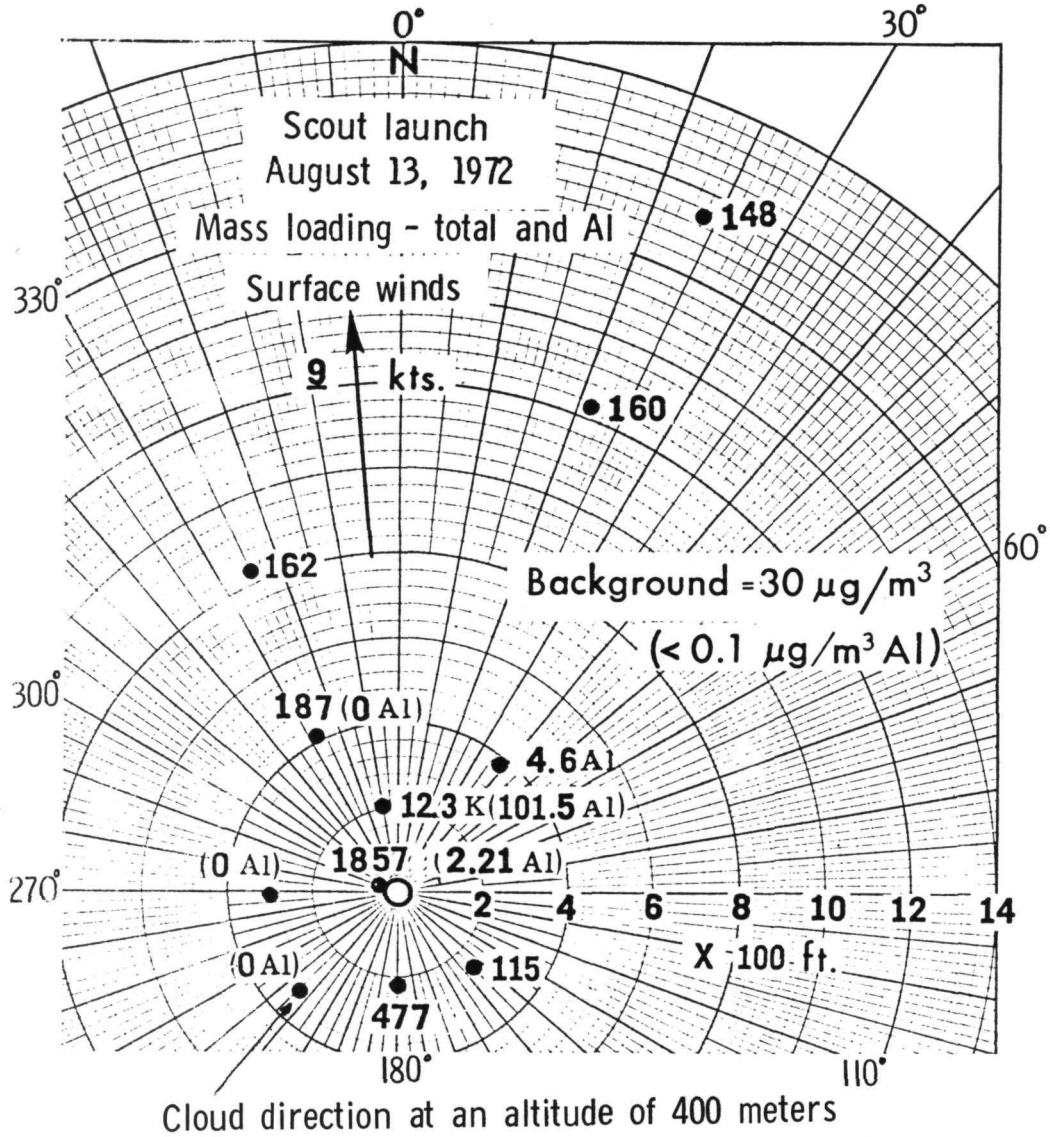

Figure 10.- Particulate mass loading ($\mu g/m^3$) collected at sites surrounding the launch point (center of polar plot) during the Scout launch.

Elemental analysis – Al

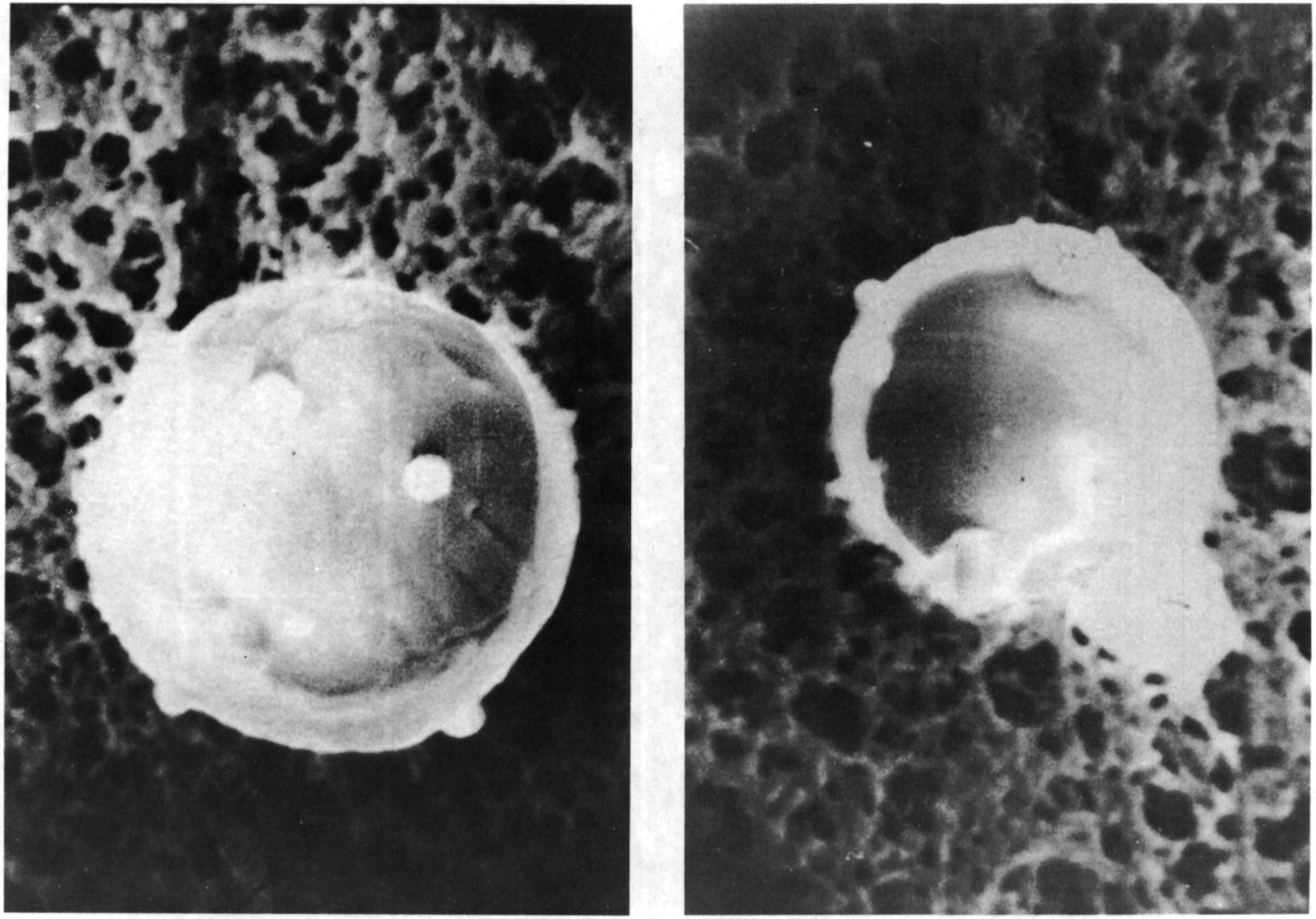

Ground site 1

Aircraft

L-74-1053

Figure 11.- SEM photographs (×10 450 magnification) of aluminum particles collected during Scout launch.

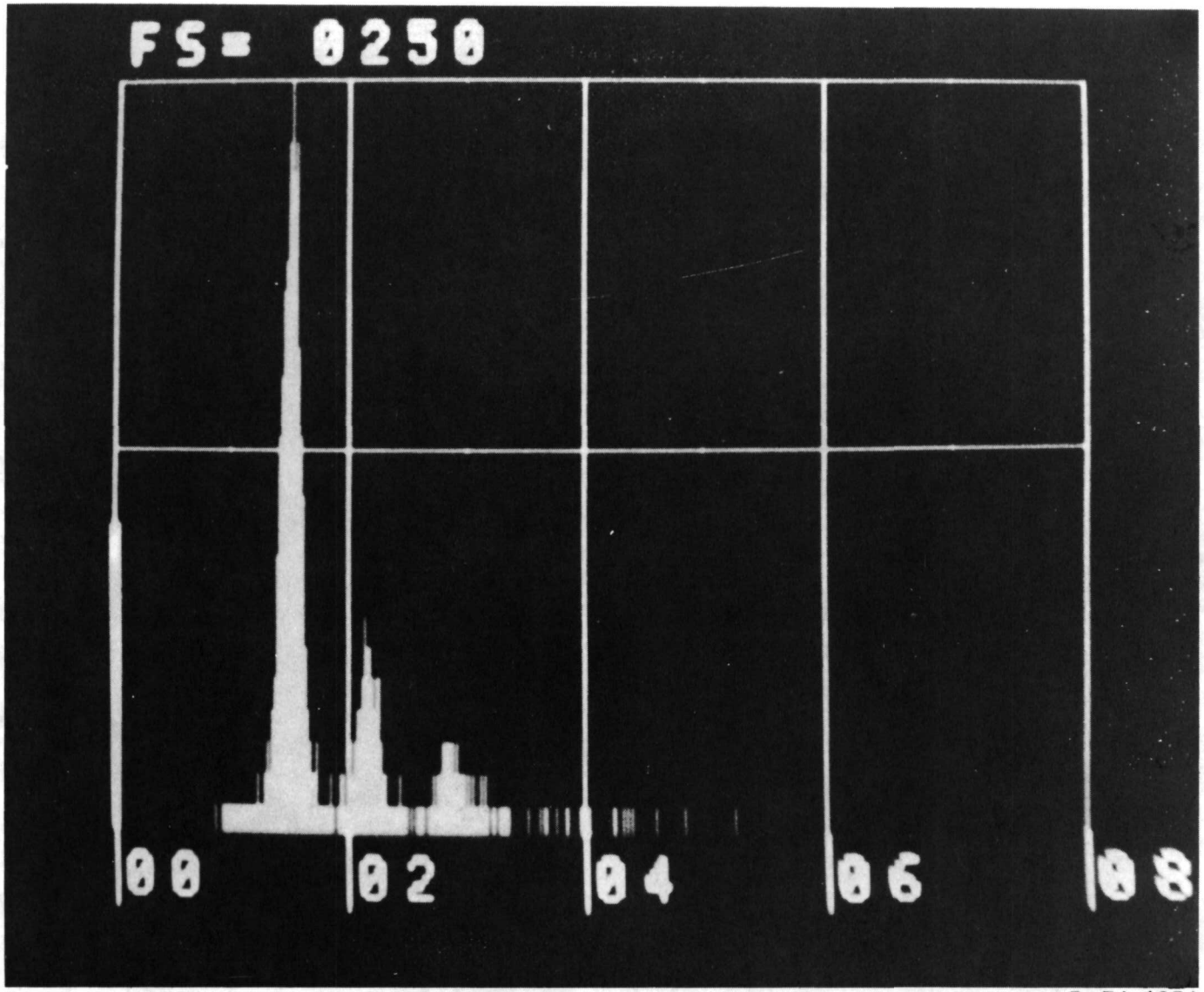

L-74-1054

Figure 12.- SEM spectra from particle in figure 11. Note large aluminum peak and small peaks from filter material.

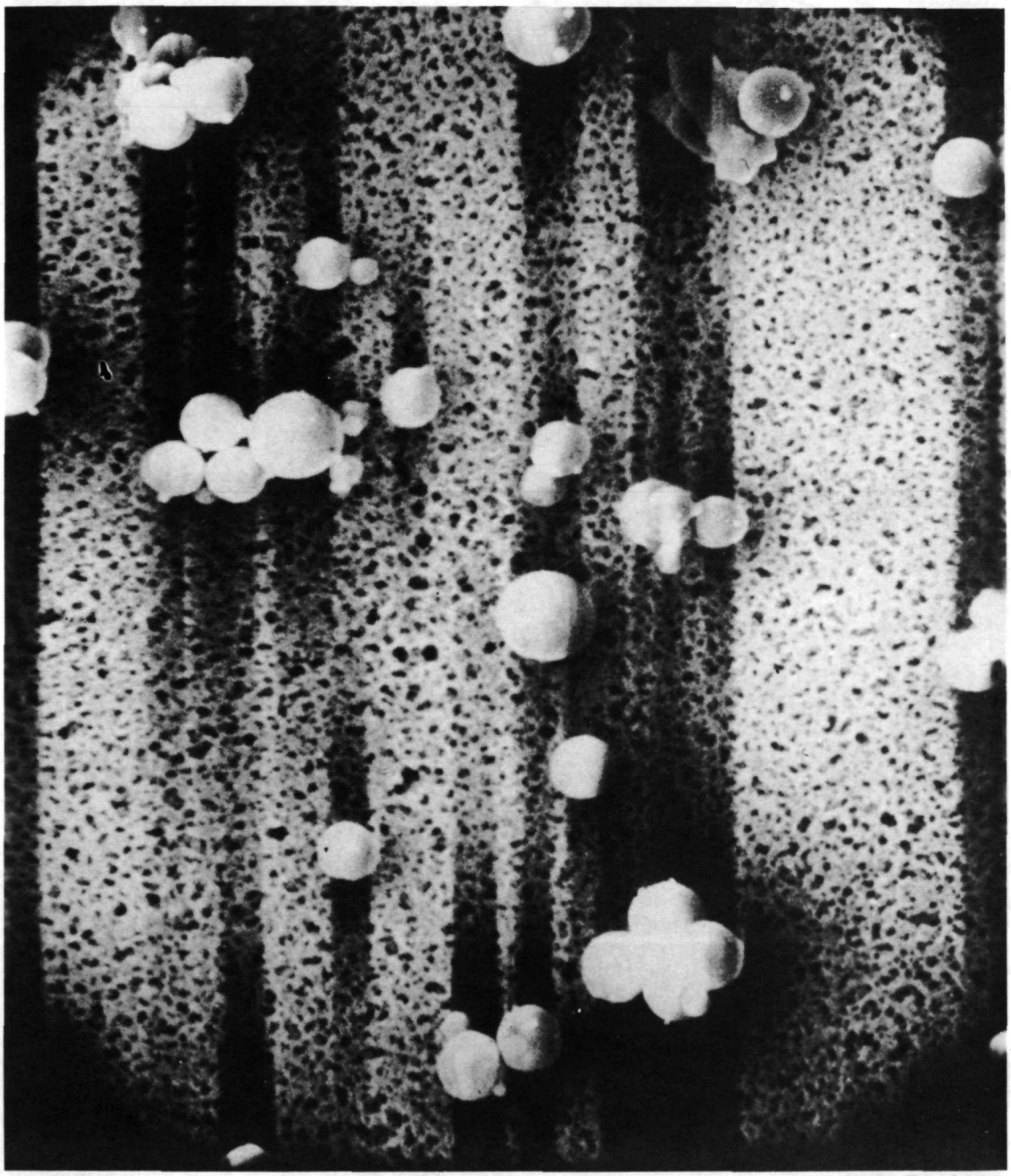

L-74-1055

Figure 13.- SEM photograph of aluminum particles with larger field of view.

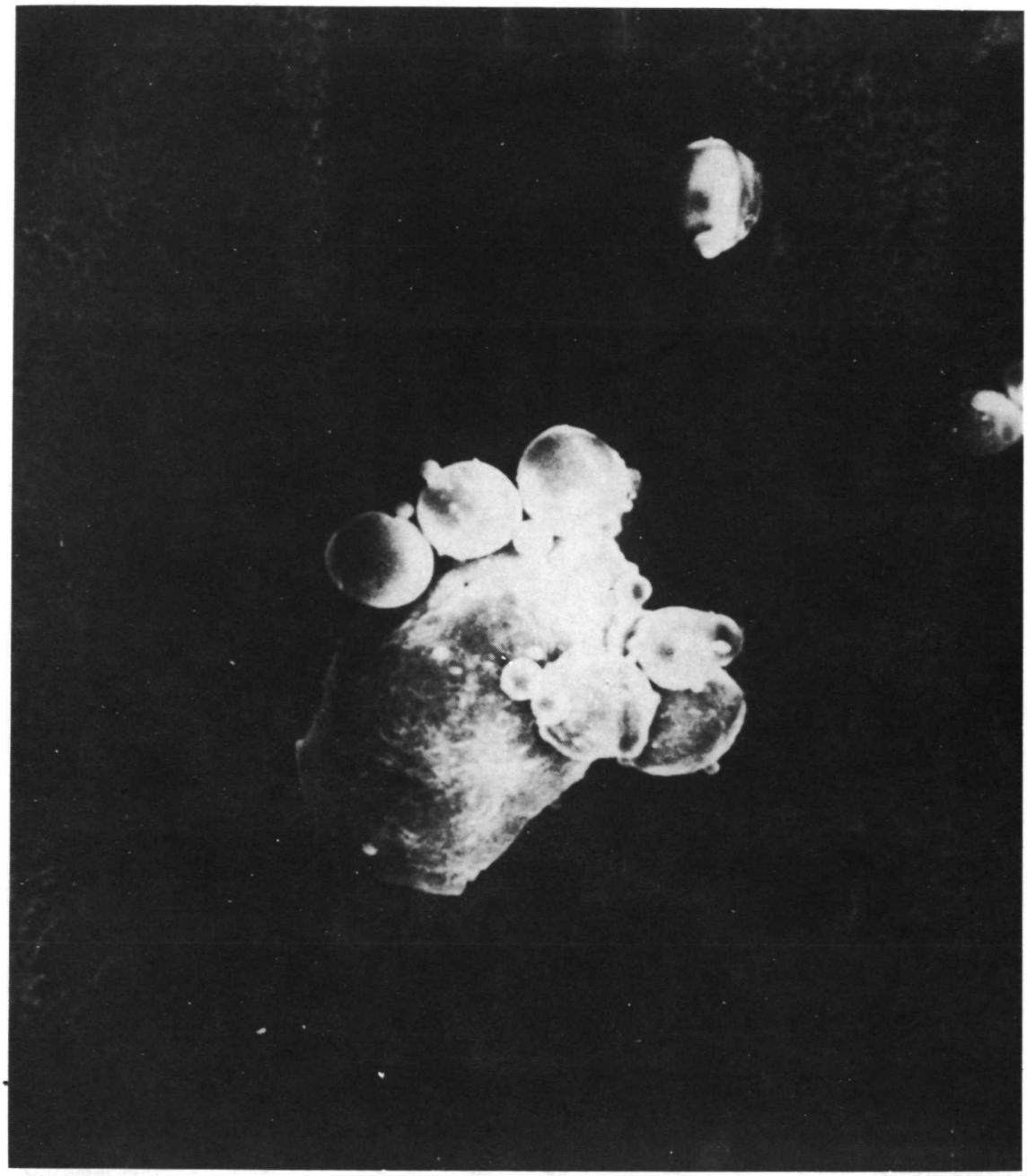

L-74-1056

Figure 14.- SEM photograph emphasizing agglomeration of some Scout exhaust particles.

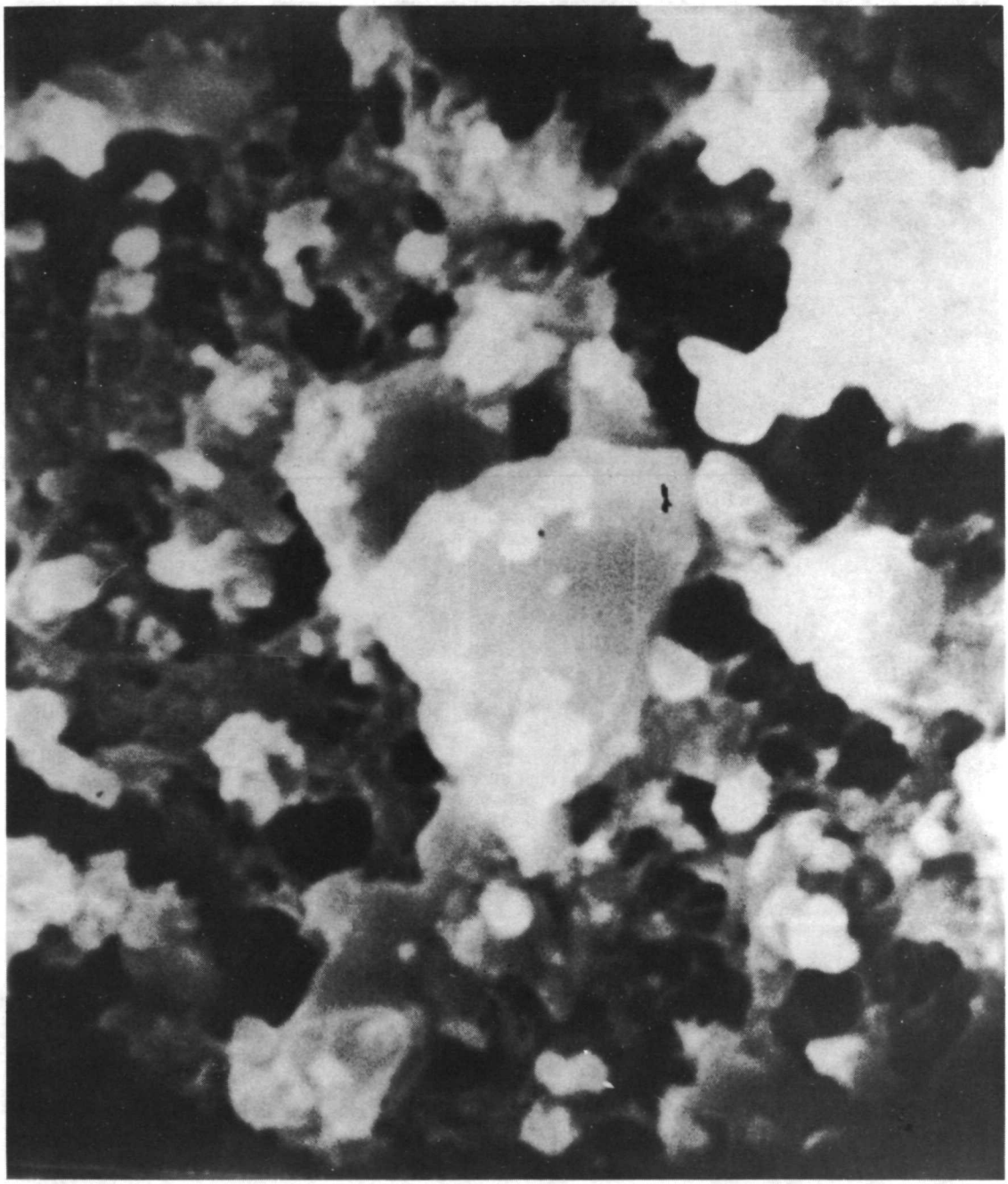

L-74-1057

Figure 15.- SEM photograph emphasizing natural atmospheric background prelaunch of Scout rocket.

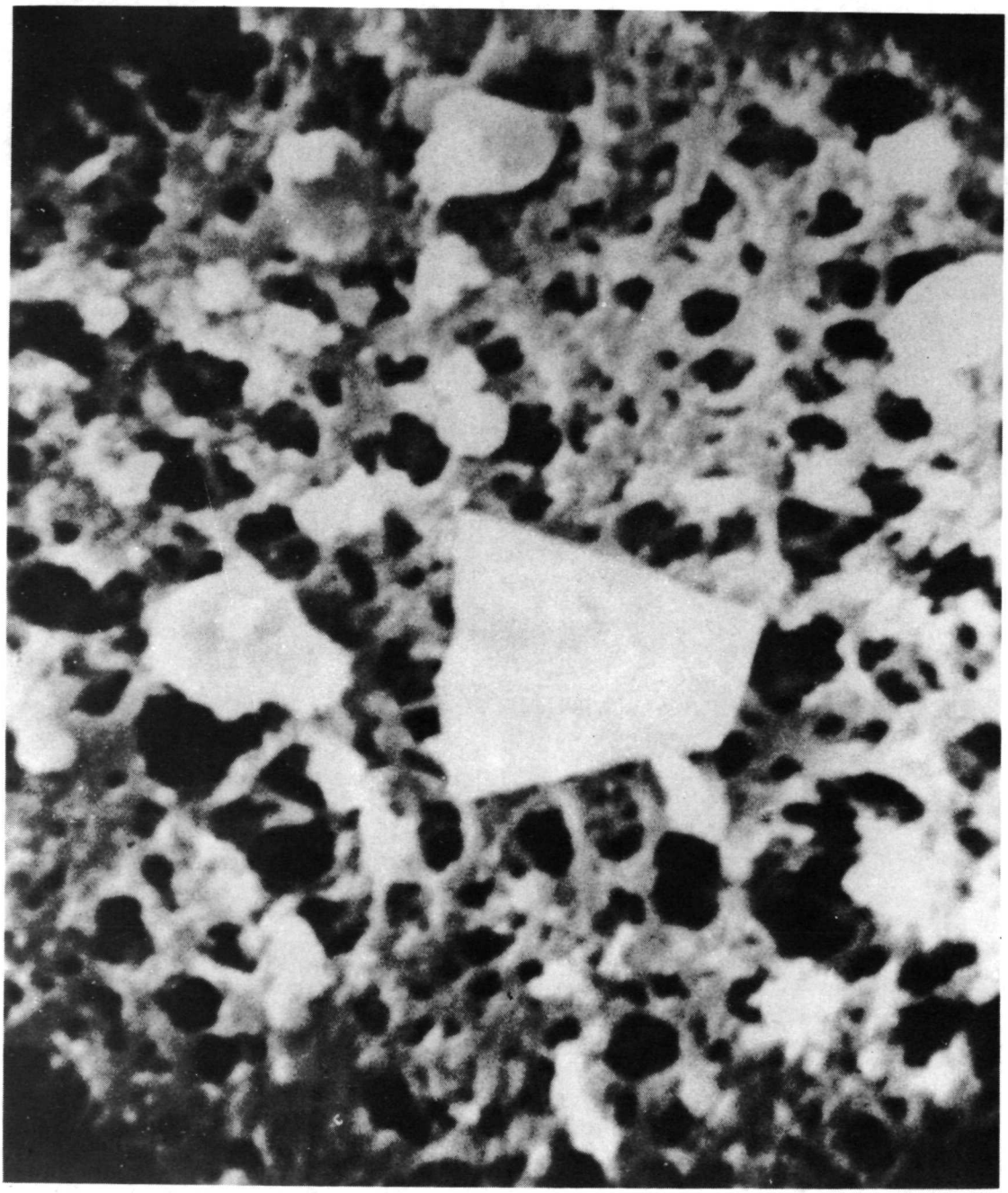

L-74-1058

Figure 16.- SEM photograph emphasizing natural atmospheric background postlaunch of Scout rocket.

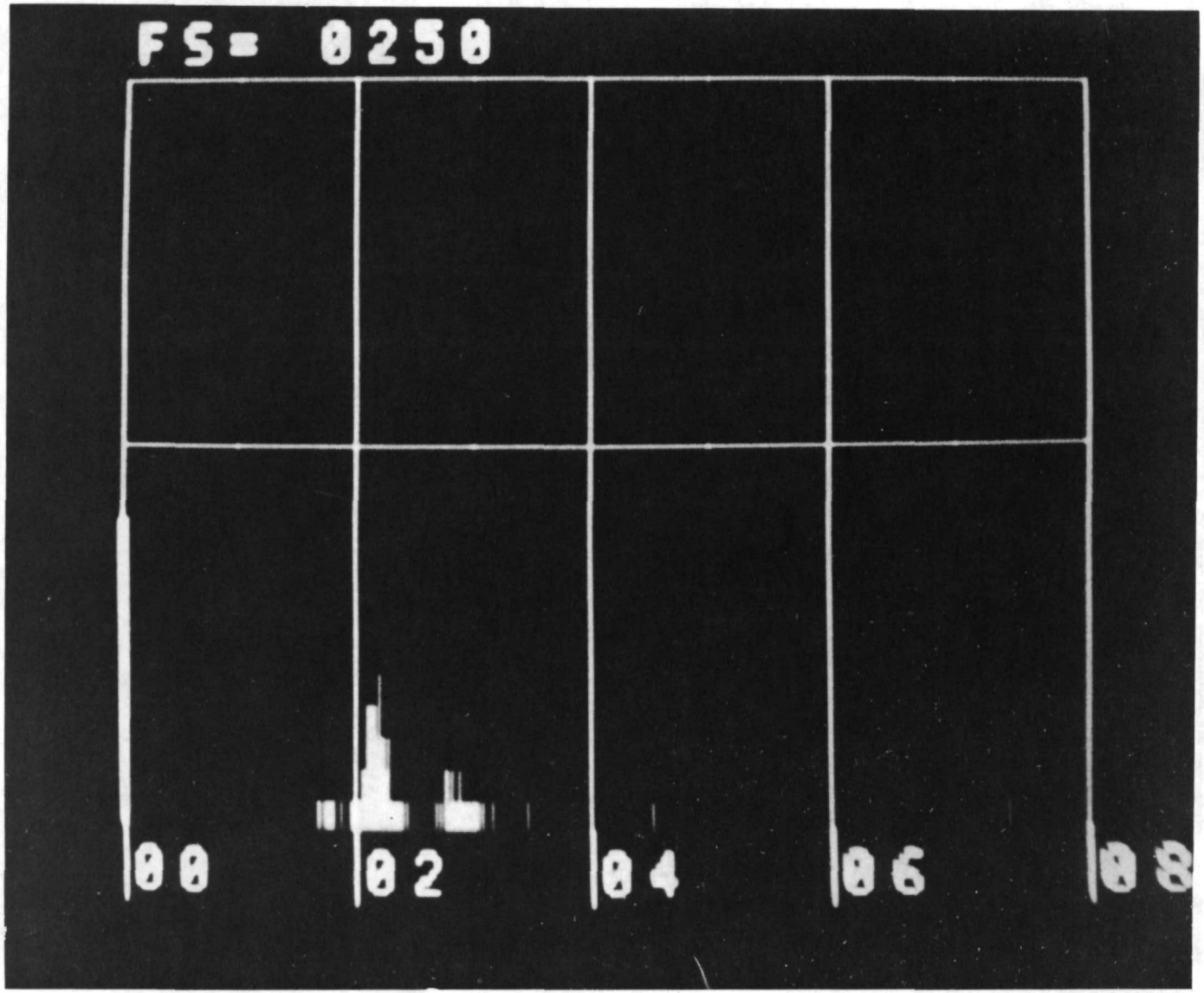

L-74-1059

Figure 17.- SEM analysis of an unexposed filter showing a phosphorous and chlorine peak.

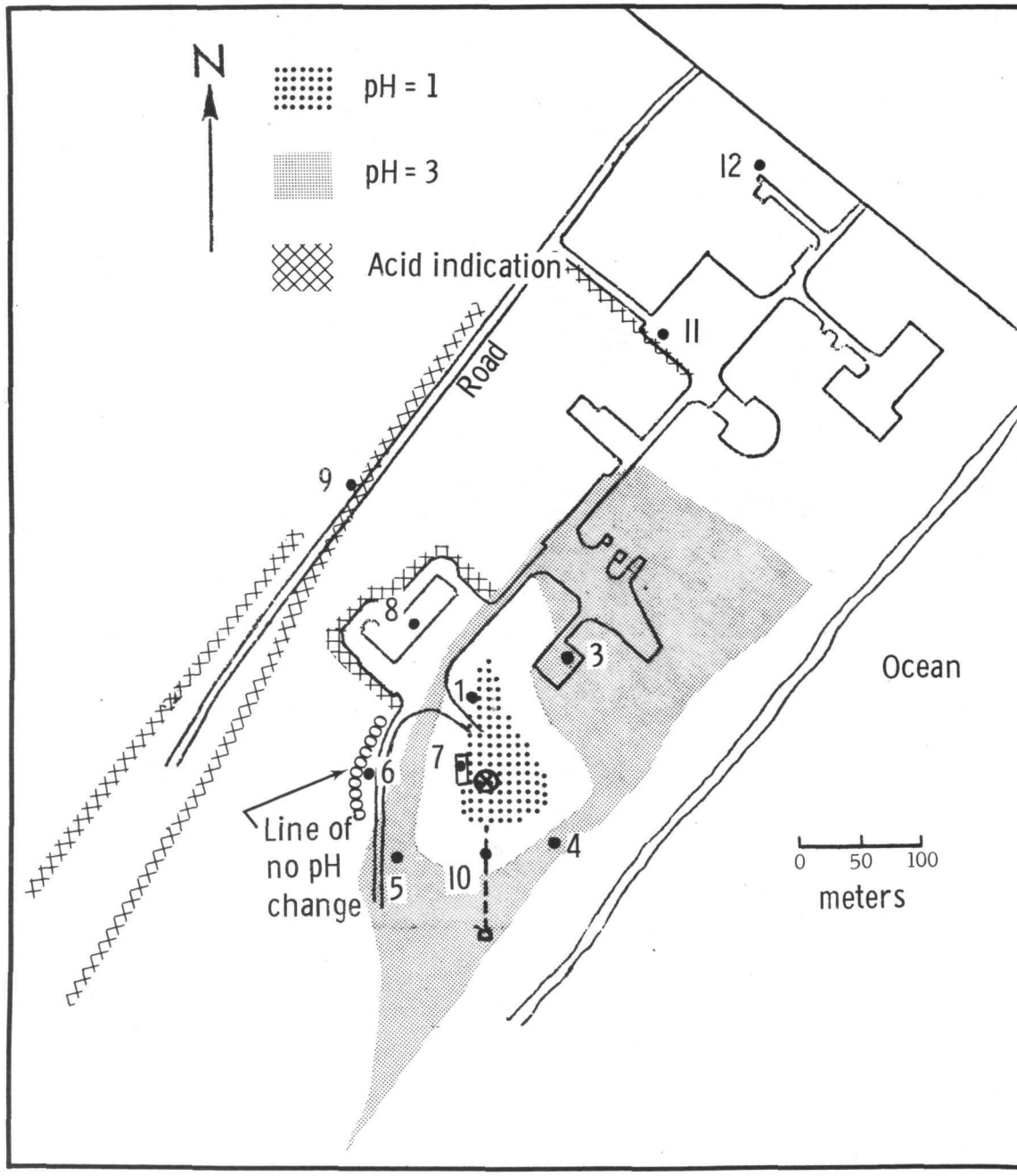

Figure 18.- pH paper results of Scout launch. Blank areas were not indicated.

Site	Distance from launch site, km	Angle from launch site, deg
MAML	0.75	111
0	2.24	263
Q	2.57	239
R	2.76	225
S	3.18	209
1808	5.25	217

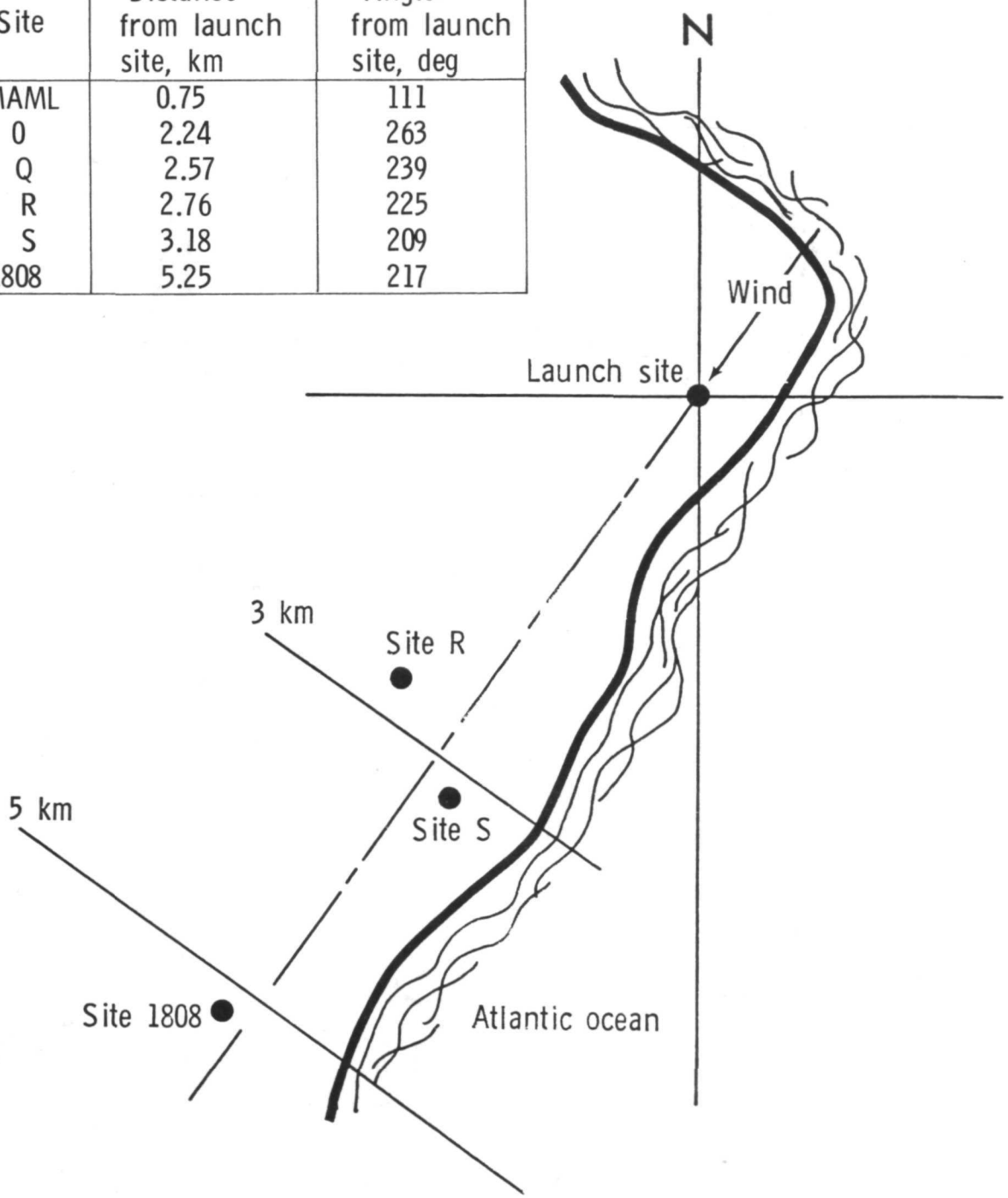

Figure 19.- Delta effluent monitoring sites at Kennedy Space Center.

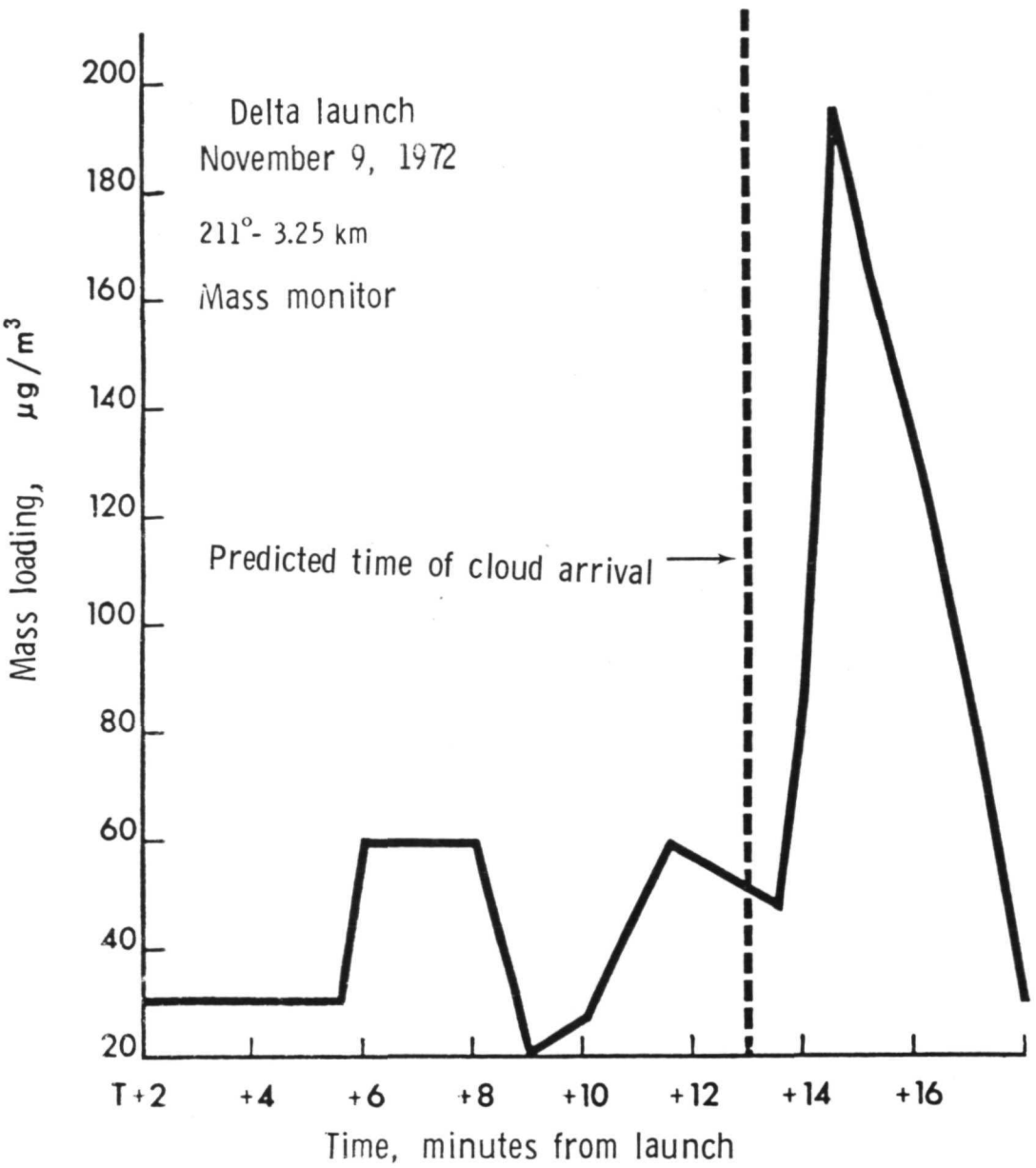

Figure 20.- Mass loading as a function of time measured by the mass monitor at site S, 318 km, 209° downwind from launch point.

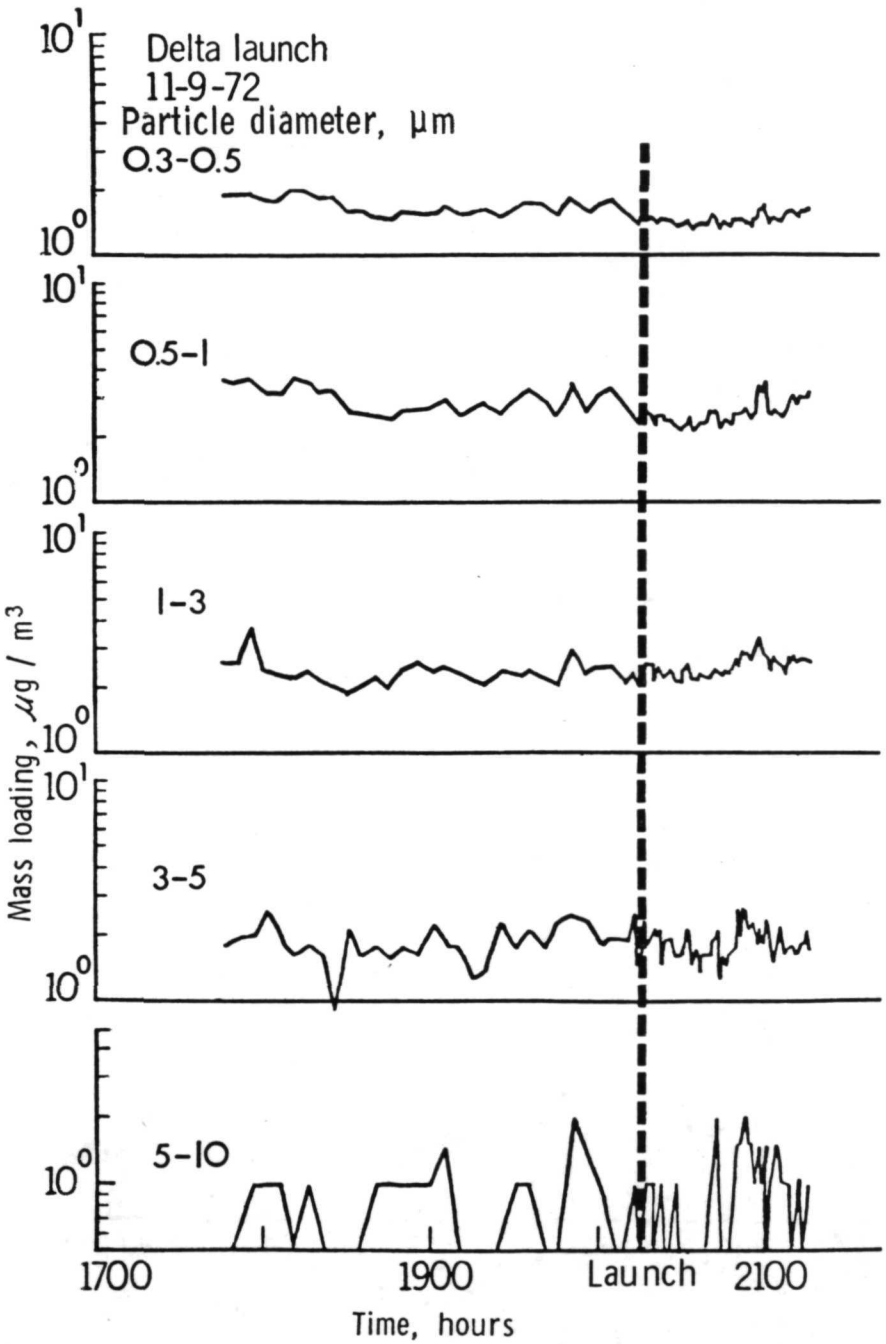

Figure 21.- Mass loading as a function of time obtained from Climet particle measurements at site R, 2.76 km, 225° downwind from launch point.

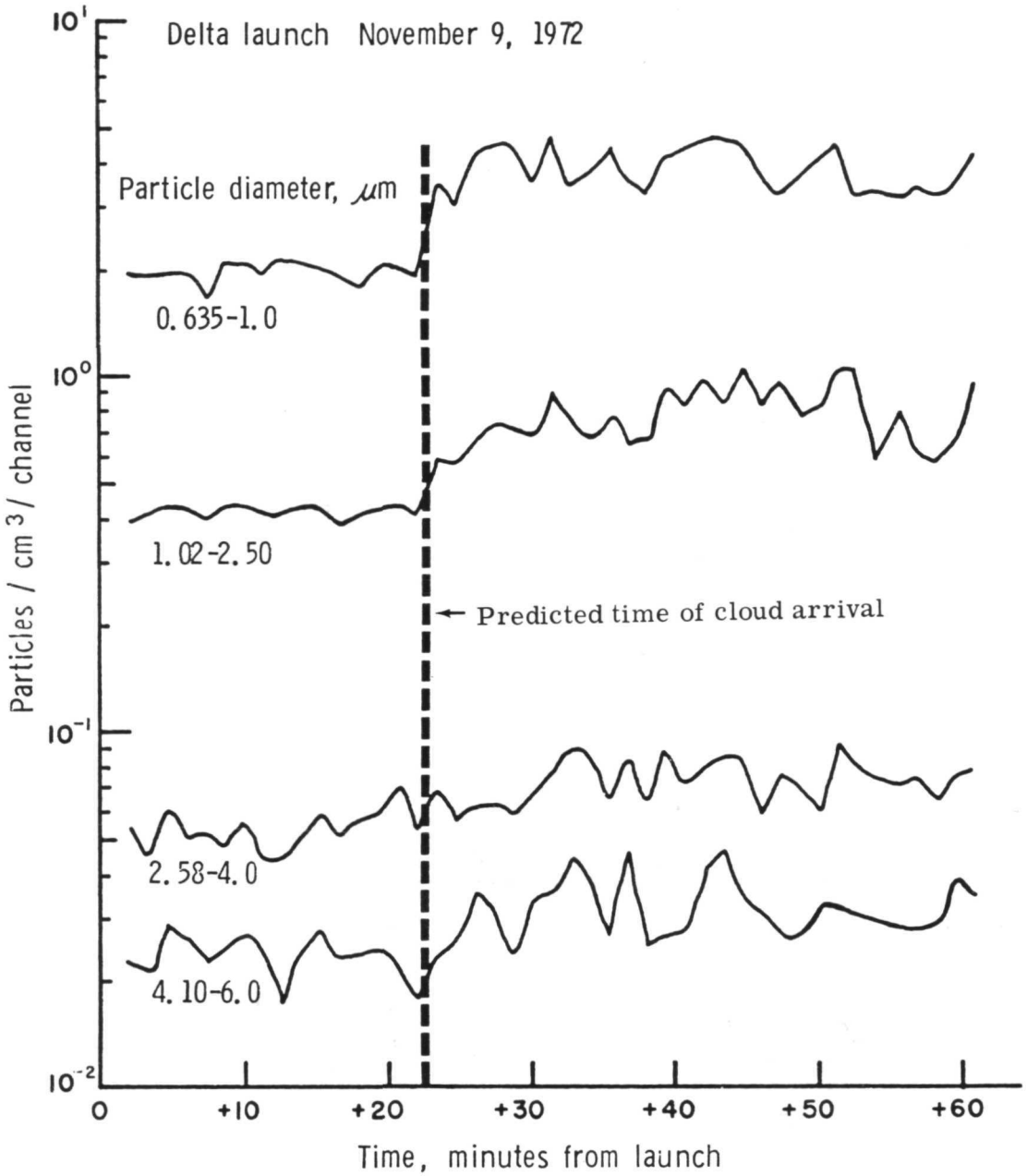

Figure 22.- Mass loading as a function of time obtained from Royco particle measurements at site 1808, 5.25 km, 217° downwind from launch point.

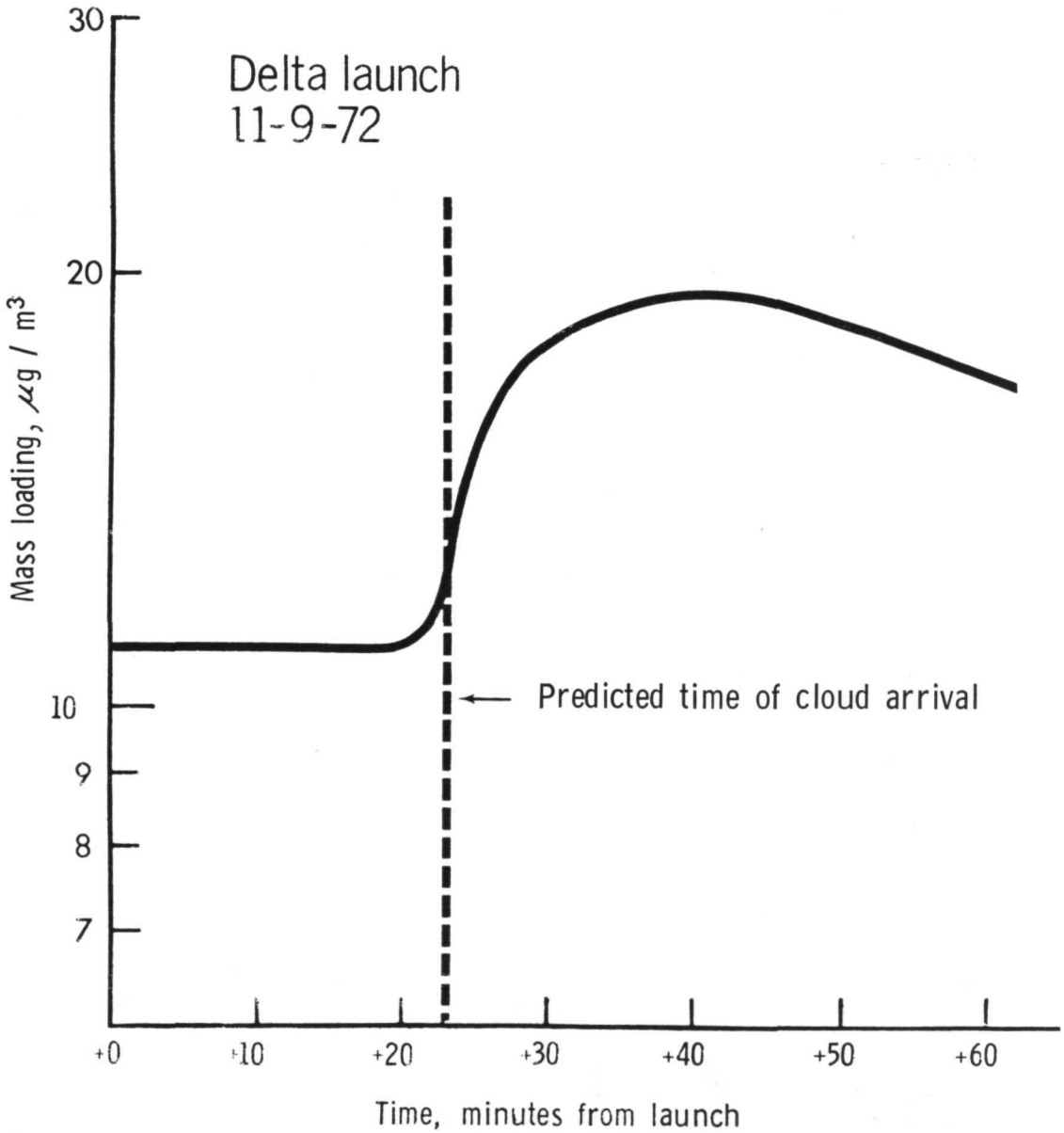

Figure 23.- Mass loading determined from total number of particles in the size range 0.6 to 6 μm, measured at site 1808, 5.25 km, 217^{o} downwind from launch point.

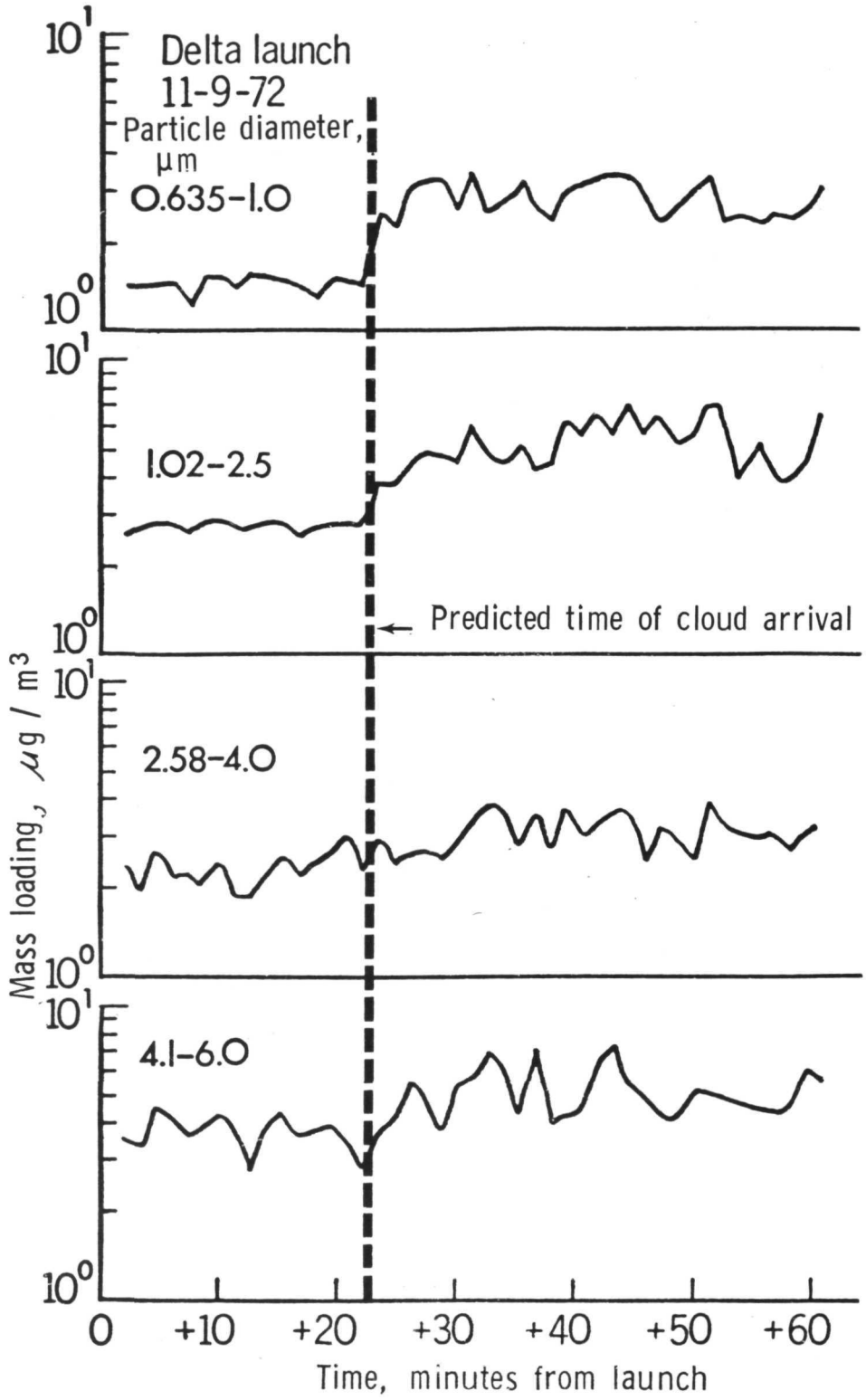

Figure 24.- Particle size distribution as a function of time measured with the Royco at site 1808, 5.25 km, 217° downwind from launch point.

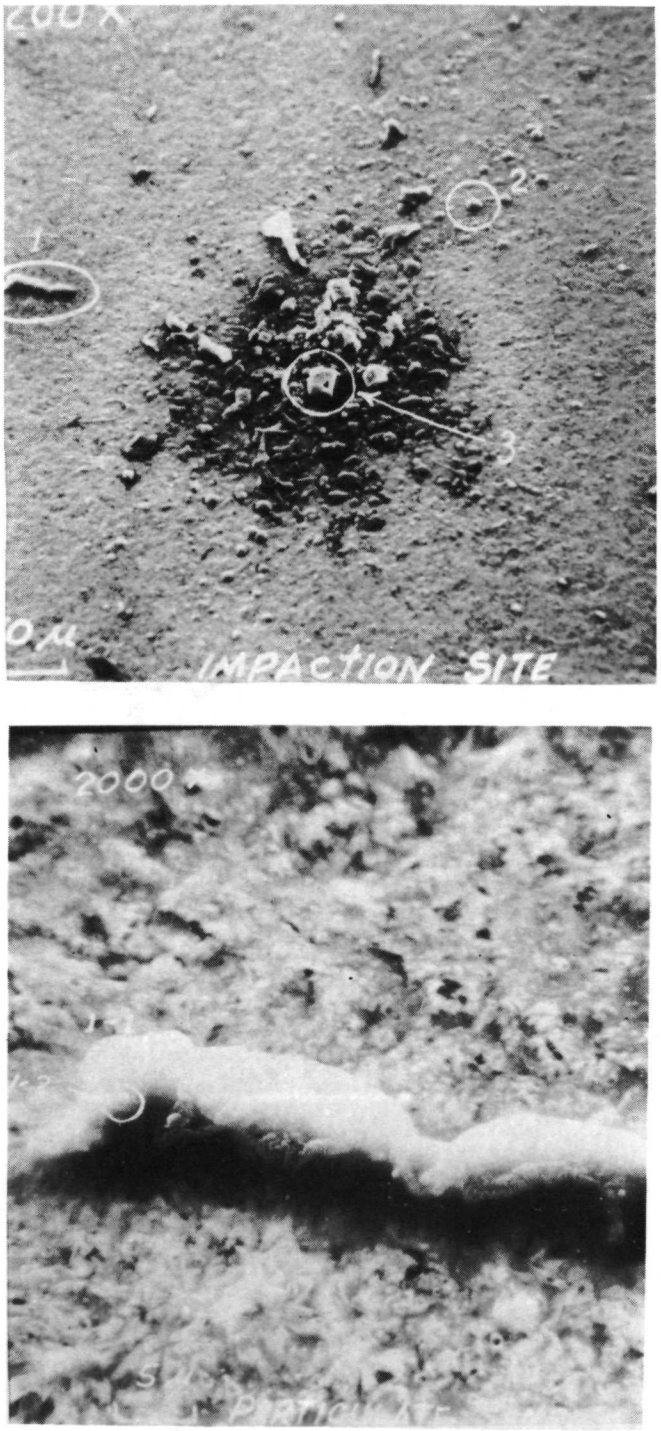

L-74-1060

(a) Particles selected for analysis and an enlargement of particle 1.

Figure 25.- SEM photomicrographs of particles collected.

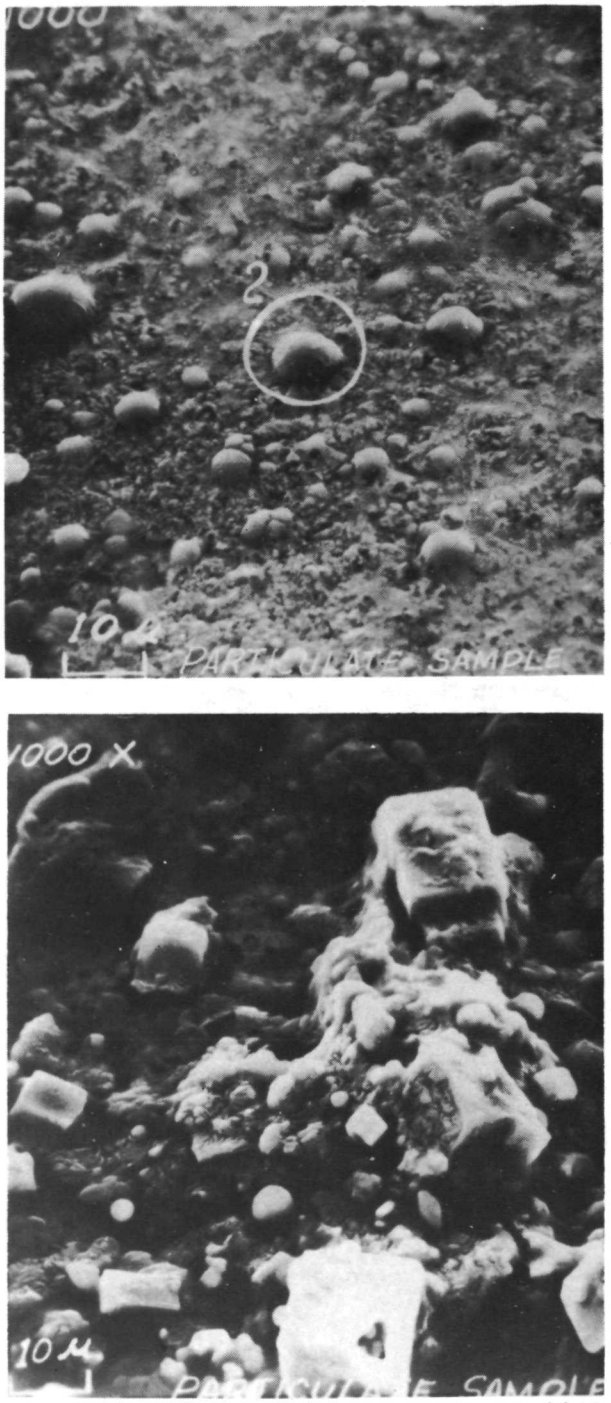

L-74-1140

(b) Enlargements of particles 2 and 3.

Figure 25.- Concluded.

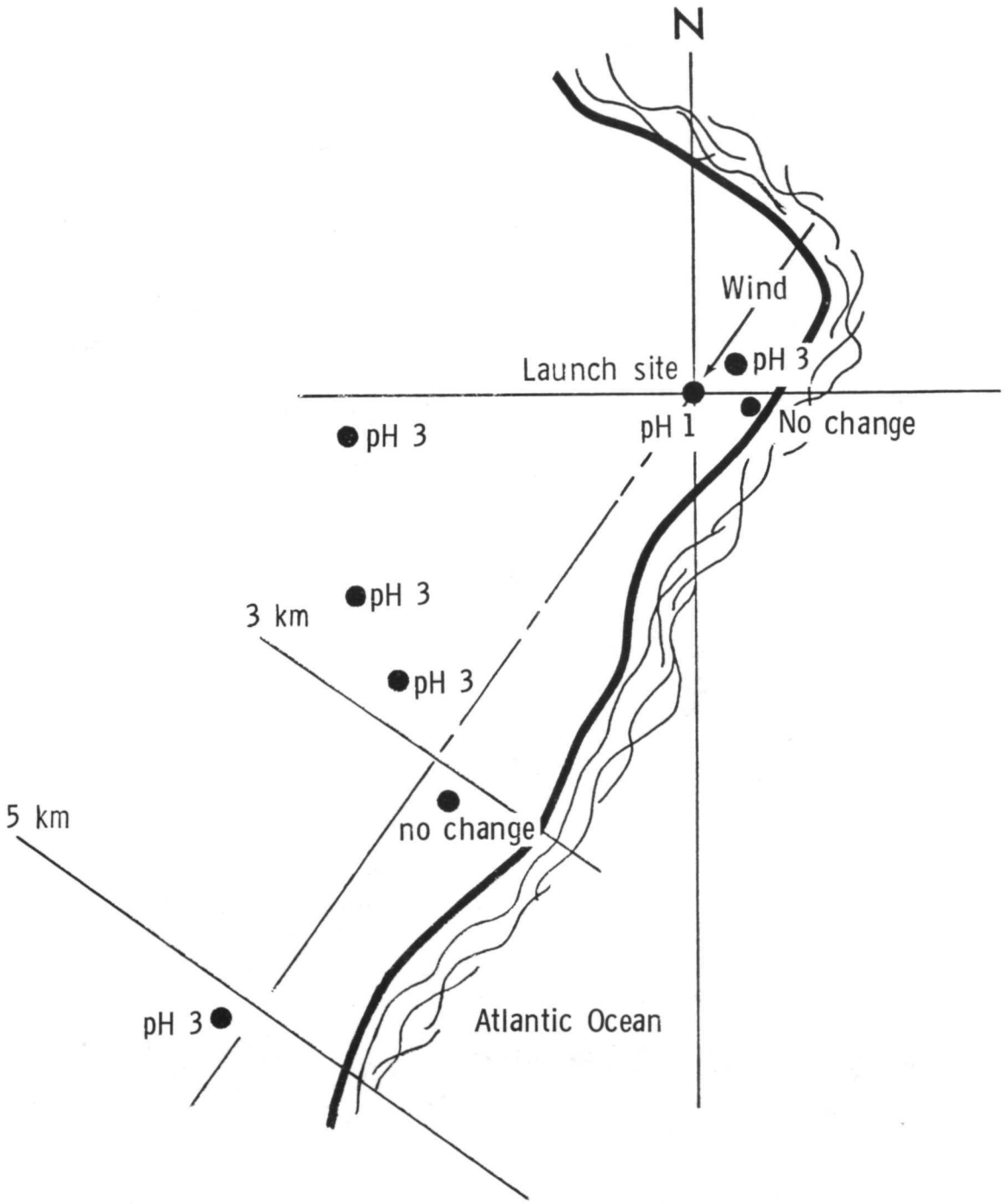

Figure 26.- Summary of pH paper locations and exposure levels.

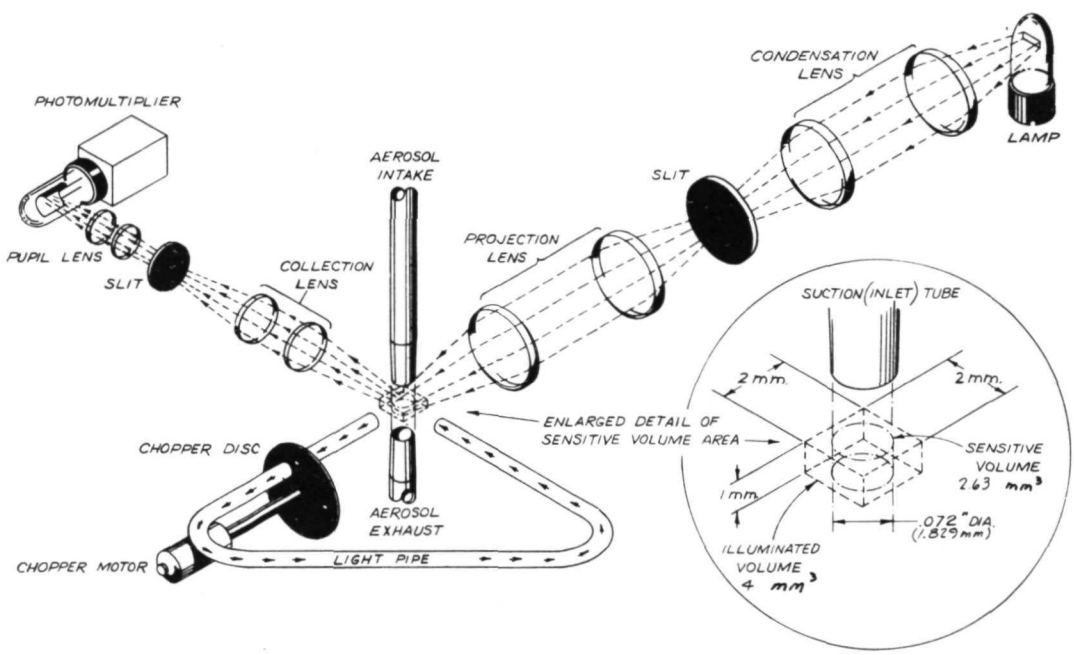

Figure 27.- Royco 220 sensor optical system (from ref. 4).

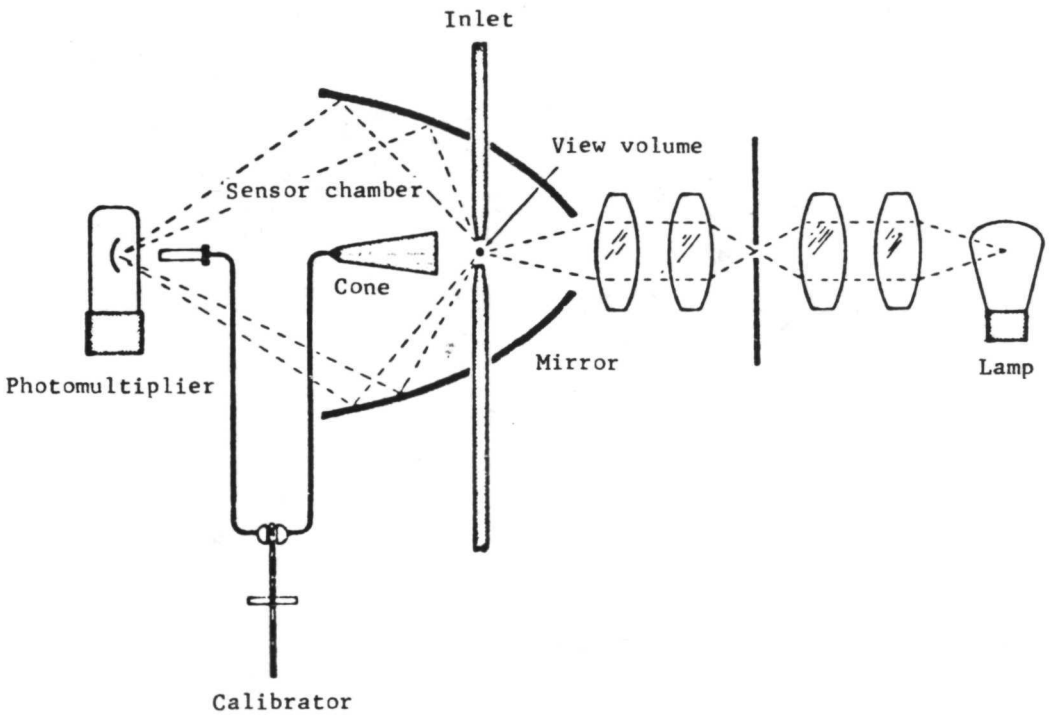

Figure 28.- Climet optical system.

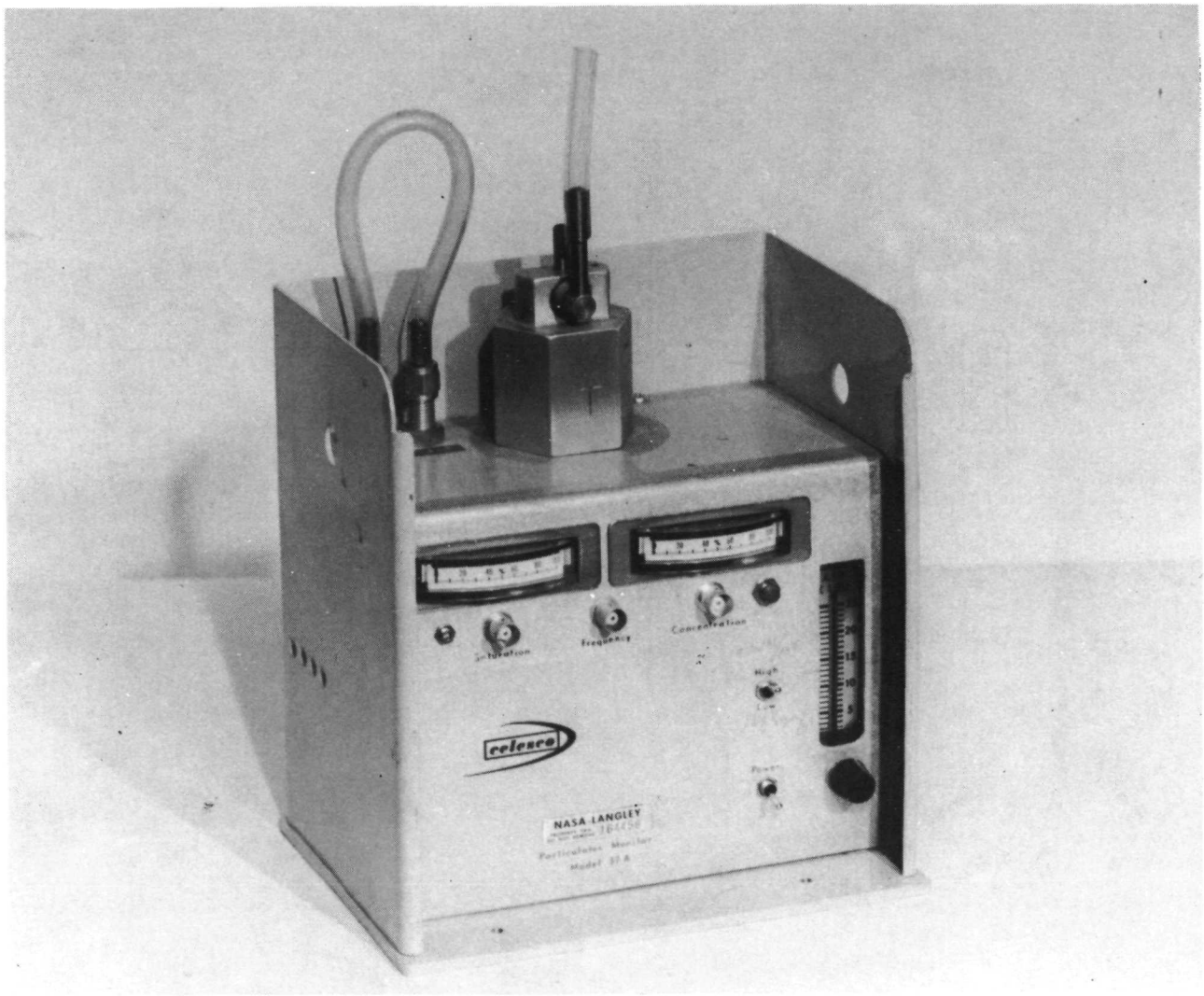

L-73-3927

Figure 29.- Celesco model 37A quartz crystal mass monitor.

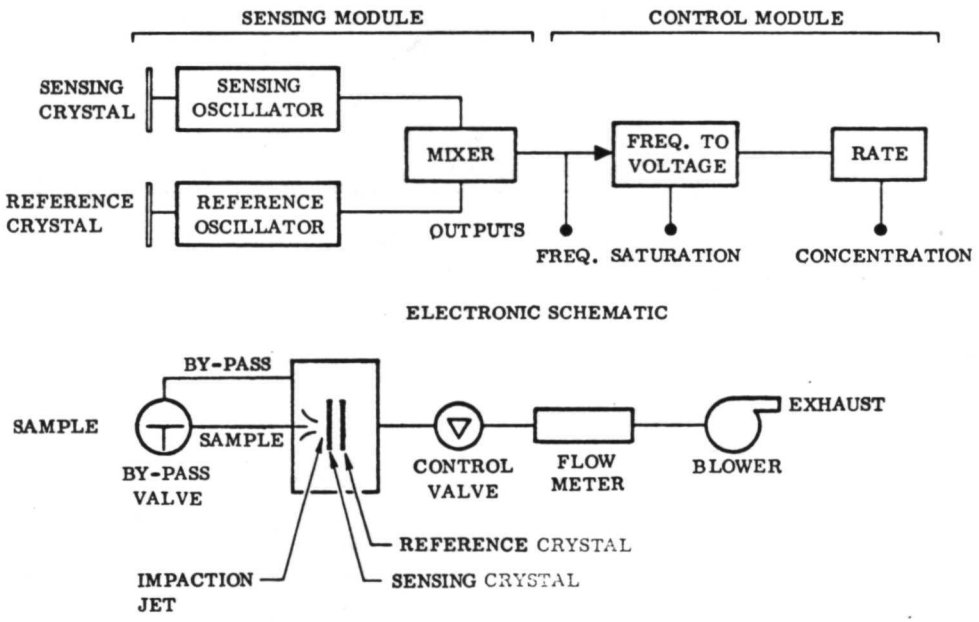

Figure 30.- Electronic schematic and flow diagram for quartz crystal mass monitor.

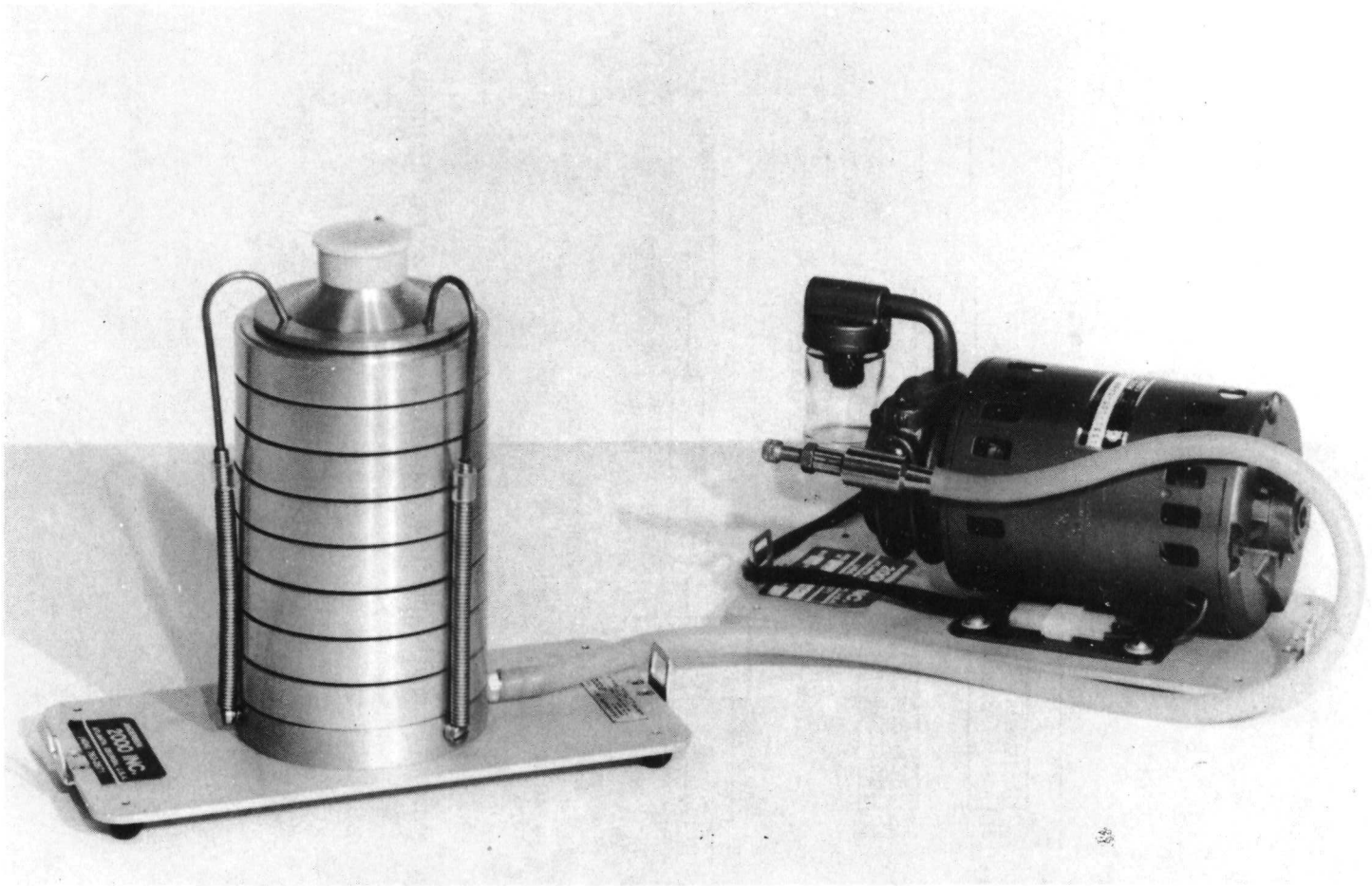

L-73-3928

Figure 31.- The Andersen impactor and pump.

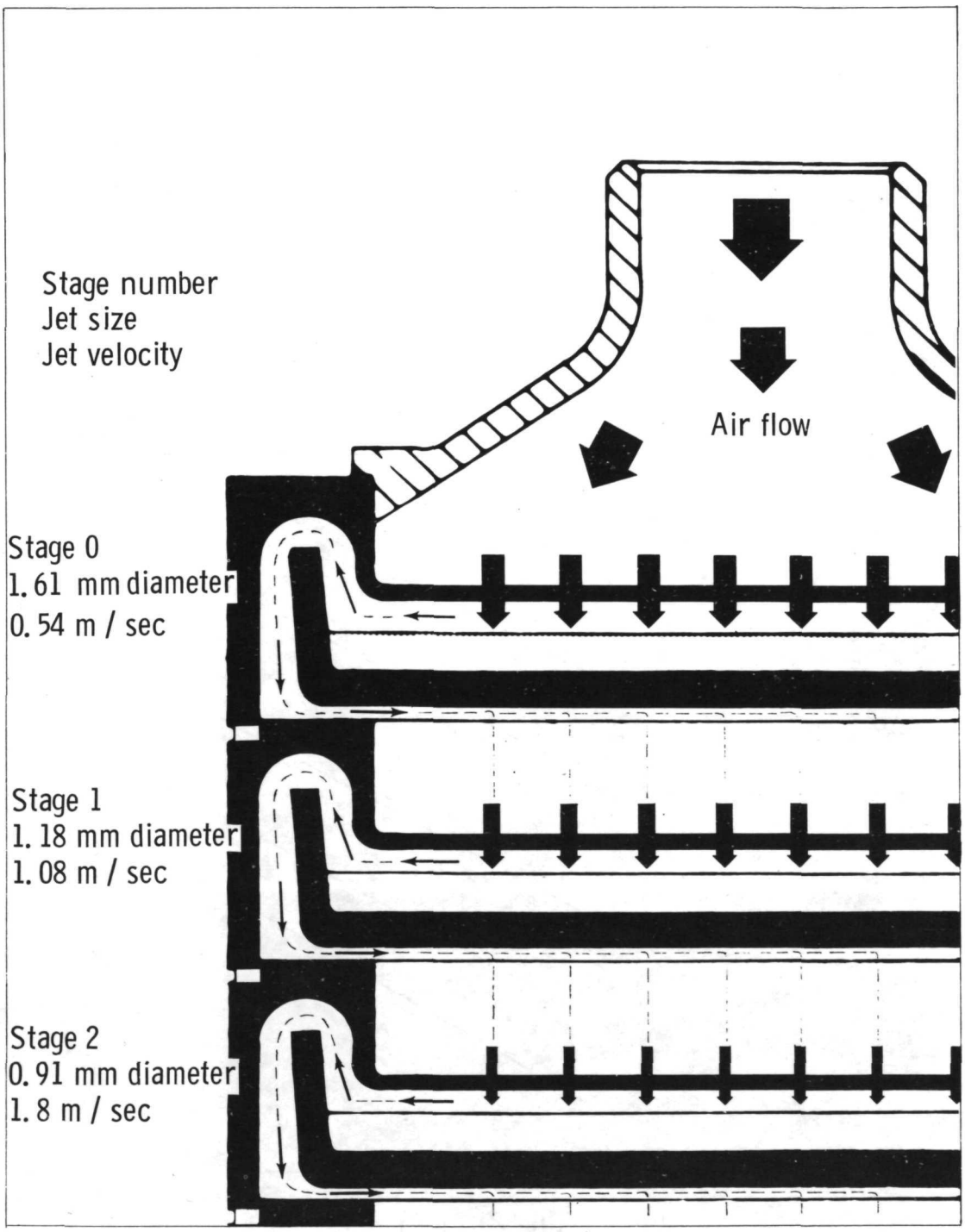

Figure 32.- Schematic flow diagram for the Andersen impactor.

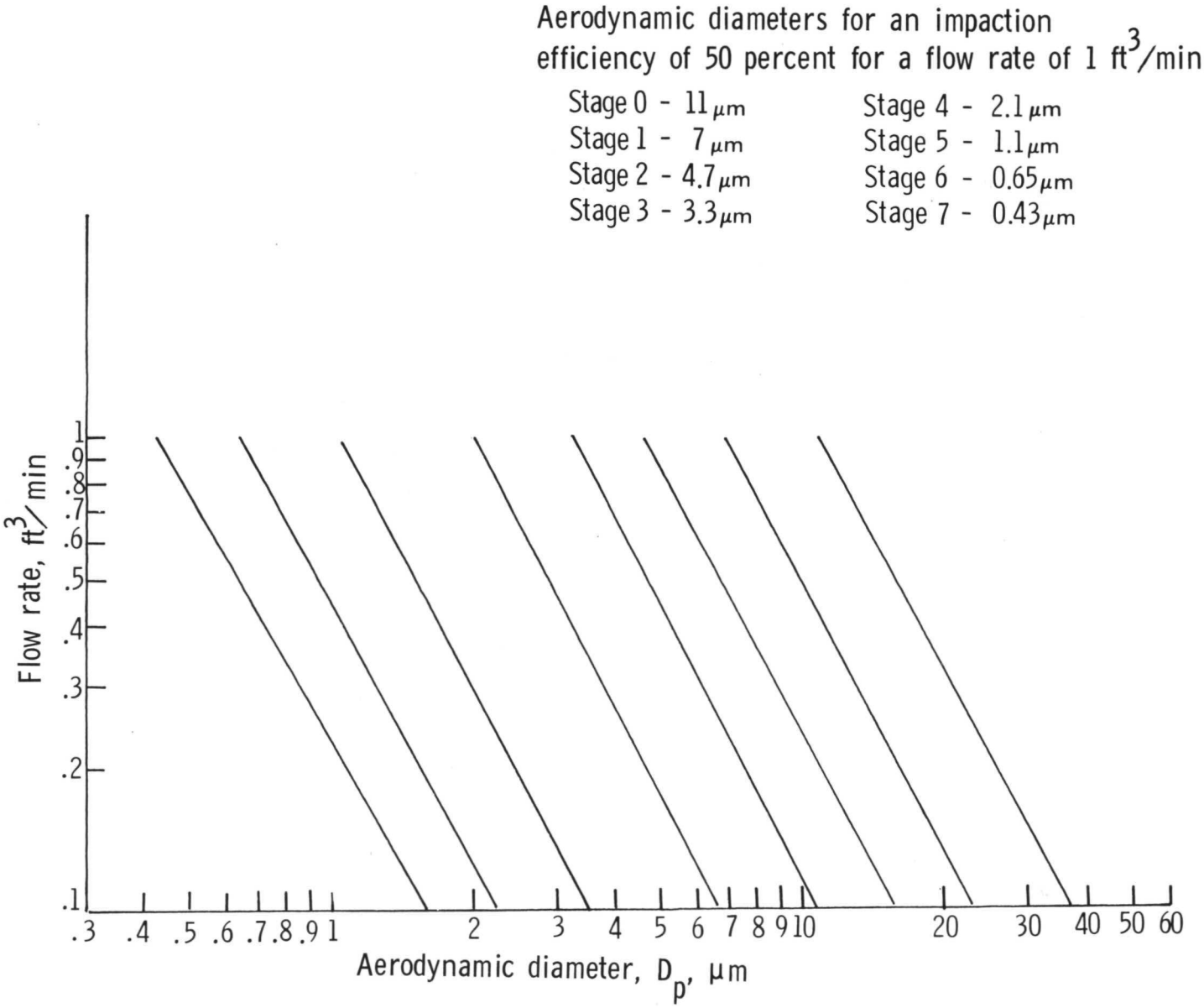

Figure 33.- Flow rate as a function of aerodynamic size for the Andersen impactor.

L-72-3559

Figure 34.- High-volume samplers:
left, with 30.48 cm (12 in.) diameter filter multistage section;
right, with 20.32 by 25.4 cm (8 by 10 in.) filter.

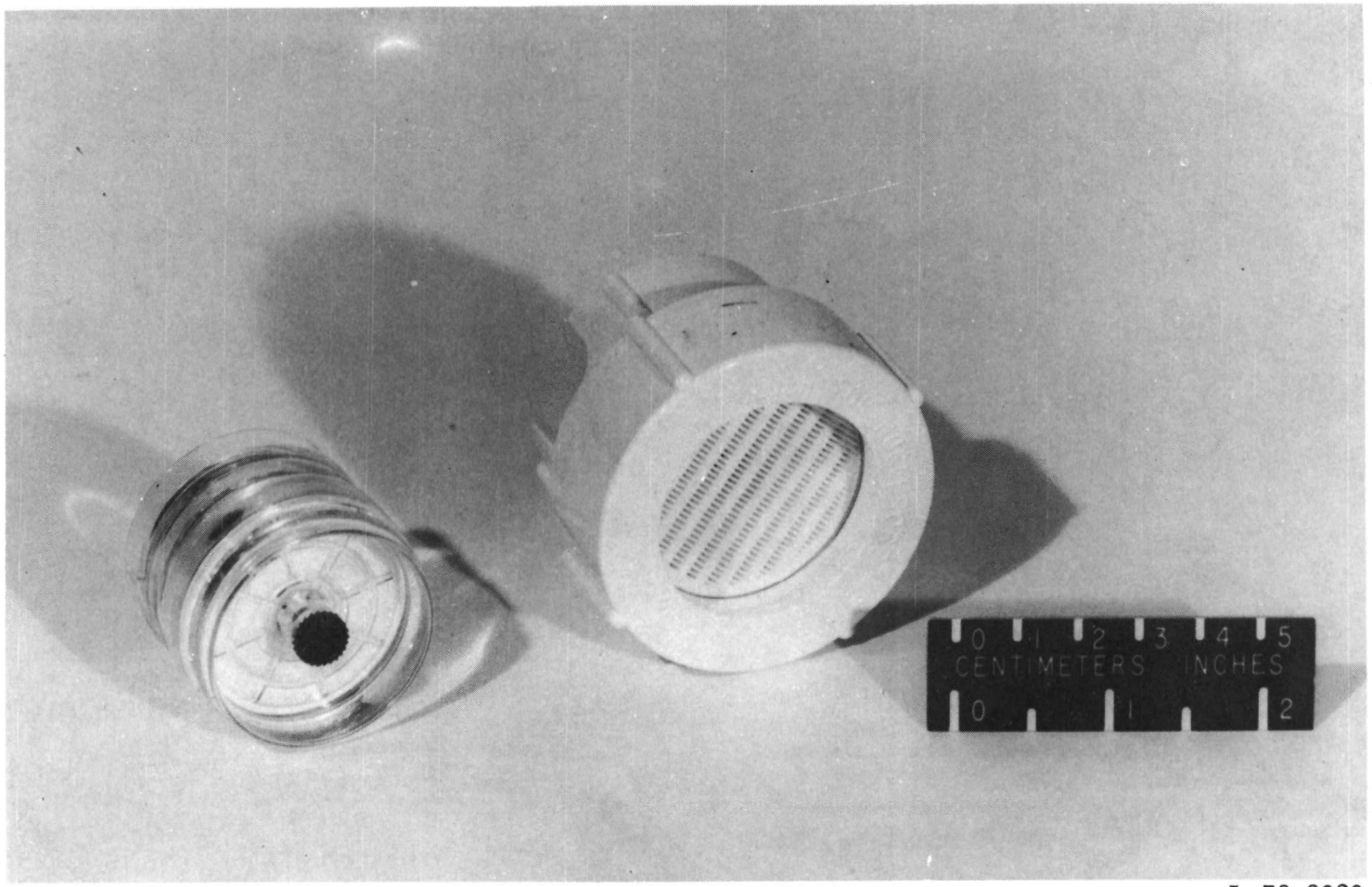

L-73-3929

Figure 35.- Membrane filter holders.

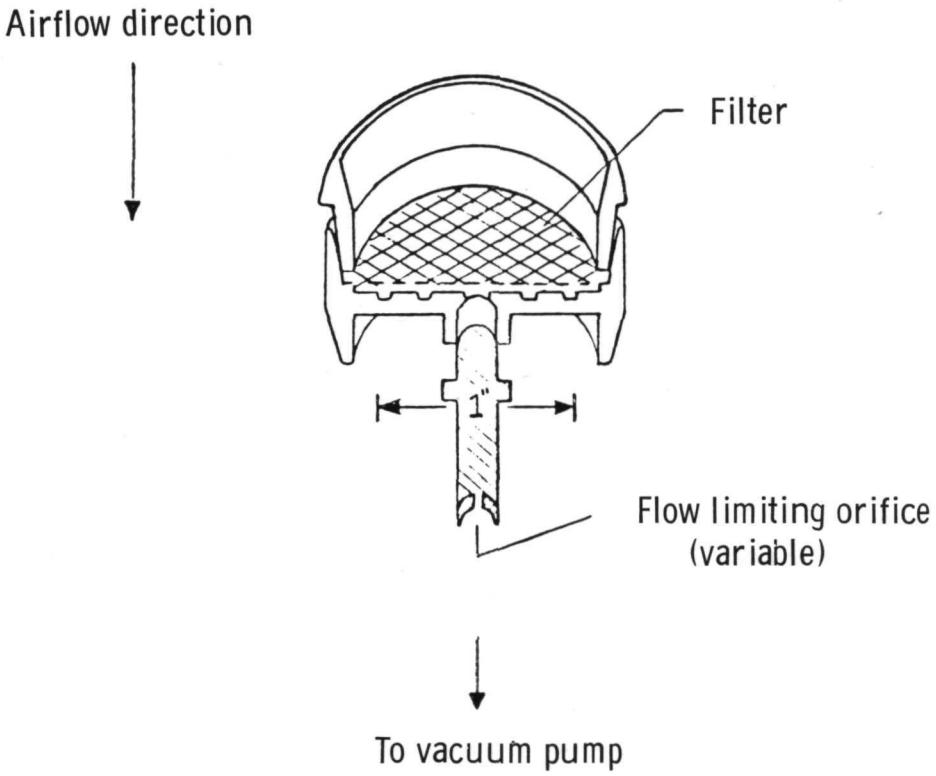

Figure 36.- Flow schematic for membrane filters.

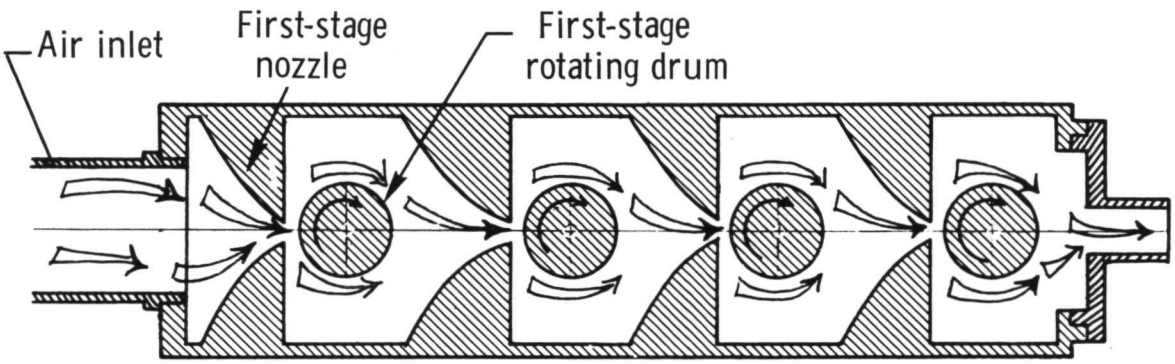

Figure 37.- Flow schematic for the Lundgren impactor.

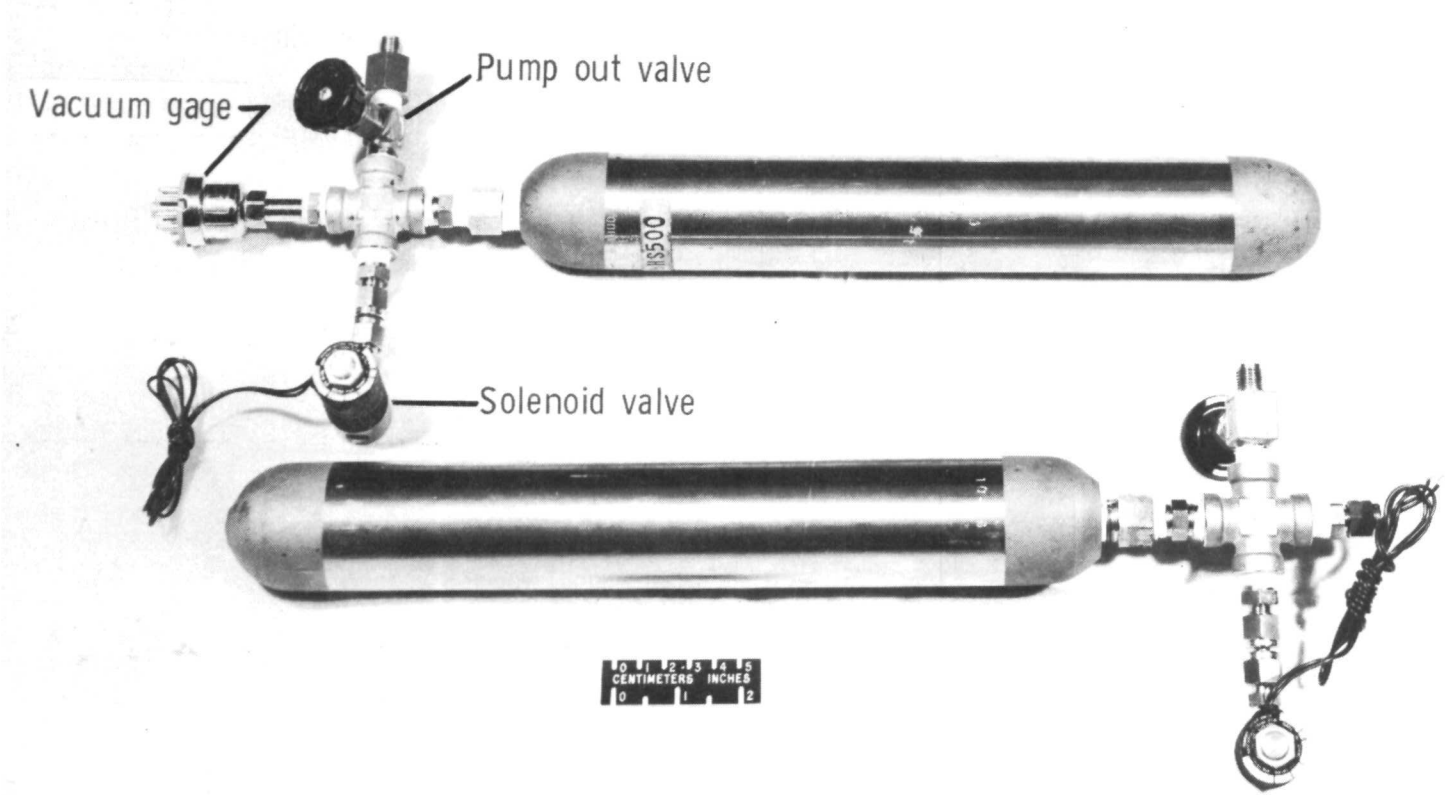

L-72-213.1

Figure 38.- 500 cm^3 gas sample cylinders.

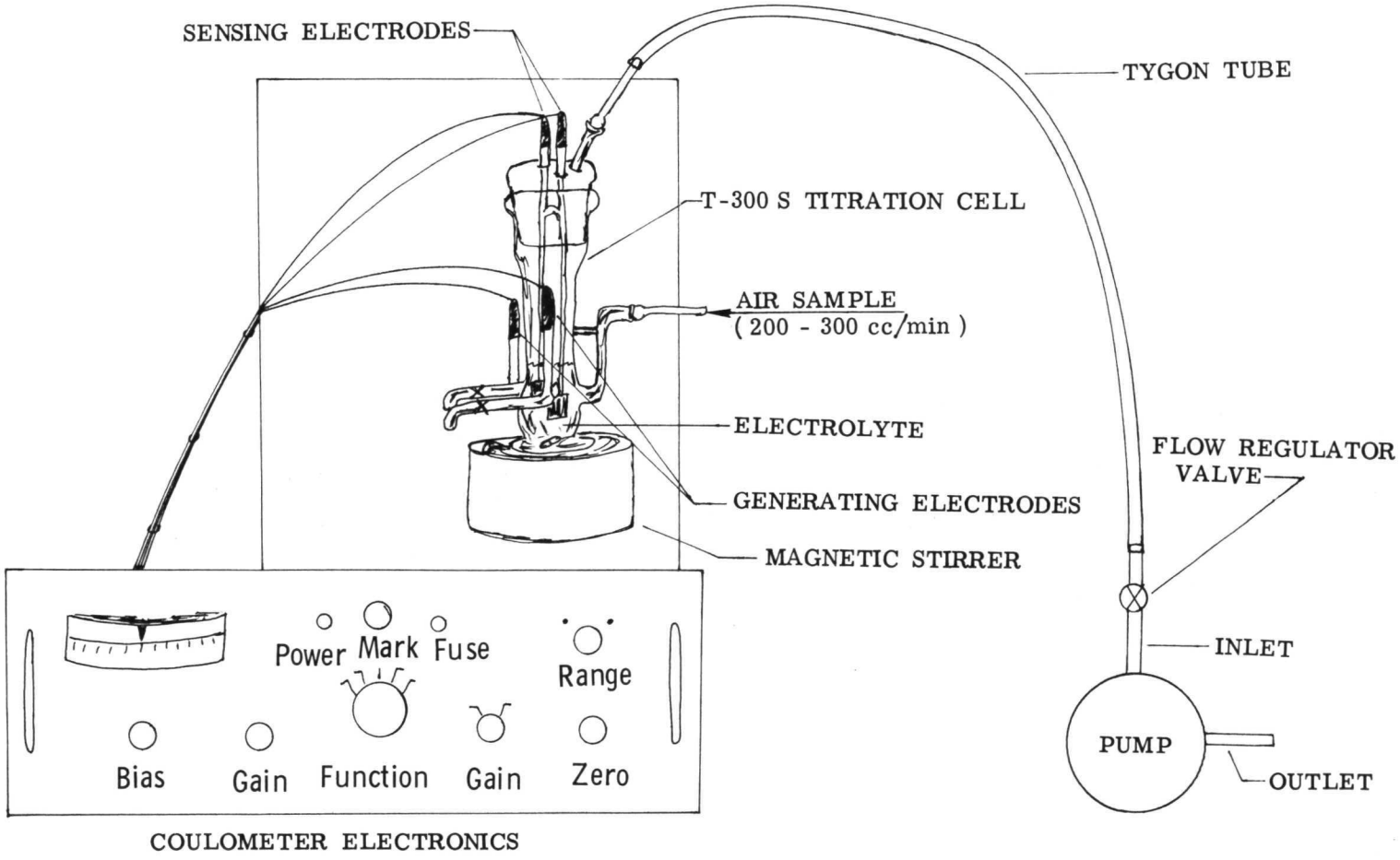

Figure 39.- Microcoulometer sampling system.

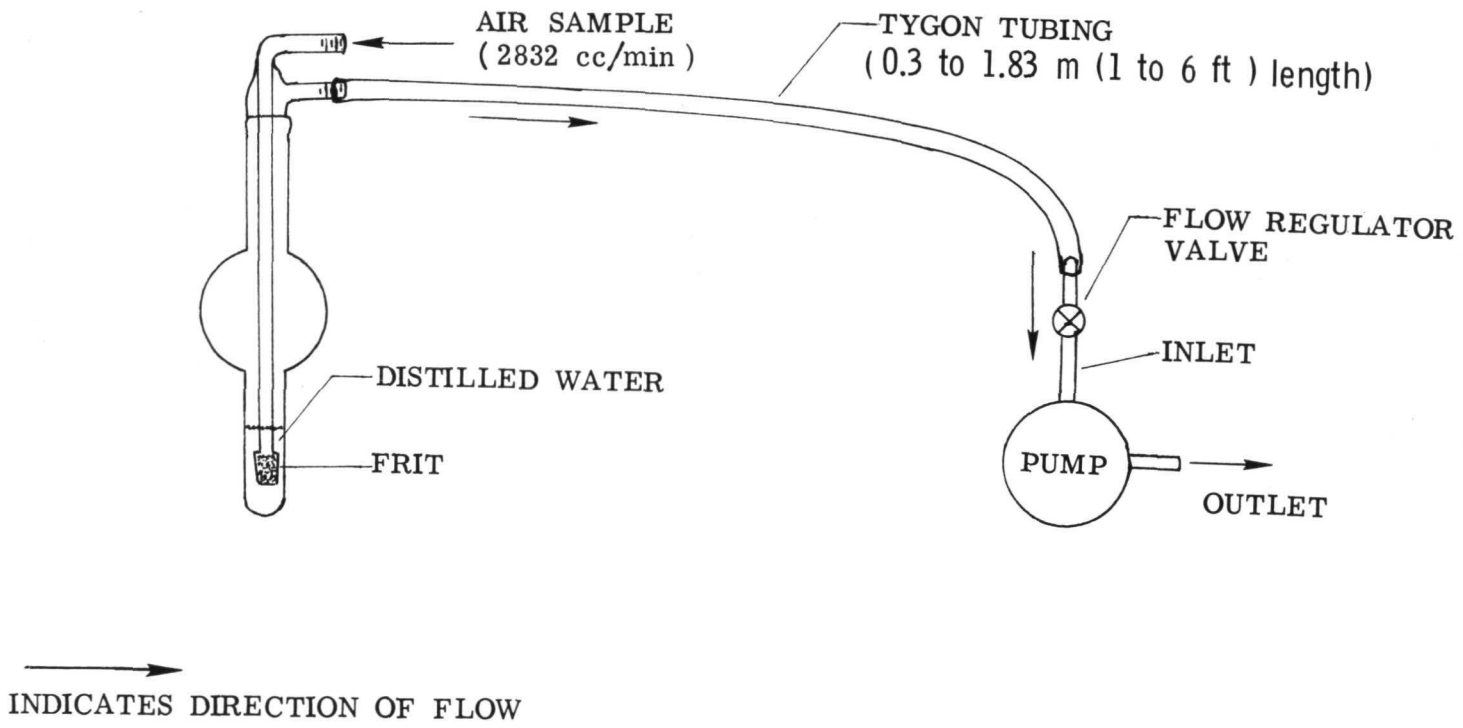

Figure 40.- Bubbler sampling system.

Page Intentionally Left Blank

Page Intentionally Left Blank

NATIONAL AERONAUTICS AND SPACE ADMINISTRATION
WASHINGTON, D.C. 20546

OFFICIAL BUSINESS
PENALTY FOR PRIVATE USE $300

SPECIAL FOURTH-CLASS RATE BOOK

POSTAGE AND FEES PAID
NATIONAL AERONAUTICS AND SPACE ADMINISTRATION
451

U.S.MAIL

POSTMASTER: If Undeliverable (Section 158 Postal Manual) Do Not Return

"The aeronautical and space activities of the United States shall be conducted so as to contribute . . . to the expansion of human knowledge of phenomena in the atmosphere and space. The Administration shall provide for the widest practicable and appropriate dissemination of information concerning its activities and the results thereof."

—NATIONAL AERONAUTICS AND SPACE ACT OF 1958

NASA SCIENTIFIC AND TECHNICAL PUBLICATIONS

TECHNICAL REPORTS: Scientific and technical information considered important, complete, and a lasting contribution to existing knowledge.

TECHNICAL NOTES: Information less broad in scope but nevertheless of importance as a contribution to existing knowledge.

TECHNICAL MEMORANDUMS: Information receiving limited distribution because of preliminary data, security classification, or other reasons. Also includes conference proceedings with either limited or unlimited distribution.

CONTRACTOR REPORTS: Scientific and technical information generated under a NASA contract or grant and considered an important contribution to existing knowledge.

TECHNICAL TRANSLATIONS: Information published in a foreign language considered to merit NASA distribution in English.

SPECIAL PUBLICATIONS: Information derived from or of value to NASA activities. Publications include final reports of major projects, monographs, data compilations, handbooks, sourcebooks, and special bibliographies.

TECHNOLOGY UTILIZATION PUBLICATIONS: Information on technology used by NASA that may be of particular interest in commercial and other non-aerospace applications. Publications include Tech Briefs, Technology Utilization Reports and Technology Surveys.

Details on the availability of these publications may be obtained from:

SCIENTIFIC AND TECHNICAL INFORMATION OFFICE

NATIONAL AERONAUTICS AND SPACE ADMINISTRATION

Washington, D.C. 20546